

SAM2 for Image and Video Segmentation: A Comprehensive Survey

Jiaxing Zhang Hao Tang*

Abstract—Despite significant advances in deep learning for image and video segmentation, existing models continue to face challenges in cross-domain adaptability and generalization. Image and video segmentation are fundamental tasks in computer vision with wide-ranging applications in healthcare, agriculture, industrial inspection, and autonomous driving. With the advent of large-scale foundation models, SAM2—an improved version of SAM (Segment Anything Model)—has been optimized for segmentation tasks, demonstrating enhanced performance in complex scenarios. However, SAM2’s adaptability and limitations in specific domains require further investigation. This paper systematically analyzes the application of SAM2 in image and video segmentation and evaluates its performance in various fields. We begin by introducing the foundational concepts of image segmentation, categorizing foundation models, and exploring the technical characteristics of SAM and SAM2. Subsequently, we delve into SAM2’s applications in static image and video segmentation, emphasizing its performance in specialized areas such as medical imaging and the challenges of cross-domain adaptability. As part of our research, we reviewed over 200 related papers to provide a comprehensive analysis of the topic. Finally, the paper highlights the strengths and weaknesses of SAM2 in segmentation tasks, identifies the technical challenges it faces, and proposes future development directions. This review provides valuable insights and practical recommendations for optimizing and applying SAM2 in real-world scenarios.

Index Terms—SAM2, SAM, Image Segmentation, Video Segmentation, Foundation Models, Performance Evaluation



1 INTRODUCTION

IMAGE segmentation and video segmentation are fundamental tasks in computer vision, designed to partition images or videos into meaningful regions based on semantic or spatial features [1]. These tasks have found applications in diverse fields, including healthcare [2], [3], agriculture [4], industrial inspection [5], autonomous driving [6], and satellite remote sensing [7], [8]. Image segmentation focuses on identifying and extracting target objects, boundaries, or textures from a single image, while video segmentation extends this process to the temporal dimension, aiming to segment consecutive video frames accurately while ensuring spatio-temporal consistency. Recent advances in deep learning have led to significant breakthroughs in addressing these tasks, even in complex scenarios. However, most existing models are tailored to specific imaging modalities or tasks, which limits their ability to generalize effectively across diverse domains. Consequently, developing more general and adaptable segmentation models has emerged as a critical direction for advancing the field.

The emergence of large-scale foundation models has revolutionized the research paradigm in artificial intelligence, demonstrating remarkable zero-shot and few-shot learning capabilities [9]. As a pioneering foundation model for image segmentation, SAM (Segment Anything Model) [10] has achieved notable success in natural image segmentation tasks. However, SAM faces several challenges when applied

TABLE 1: Comparative analysis of current surveys on universal image/video segmentation.

Survey	SAM2 Focus	SAM Focus	Video Segmentation	Medical Scene	Natural Scene	Year
[17]	×	✓	×	✓	×	2023
[18]	×	✓	×	✓	✓	2023
[19]	✓	×	×	✓	×	2024
[20]	✓	×	✓	×	✓	2024
[21]	×	✓	×	✓	×	2024
[22]	×	✓	✓	×	✓	2024
Ours	✓	✓	✓	✓	✓	2024

to image and video segmentation. First, because SAM’s pre-training primarily relies on natural images [11], [12], [13], it struggles to adapt effectively to other domains, resulting in reduced accuracy. Second, SAM is predominantly trained on 2D images, which limits its performance when dealing with 3D medical images and other complex data types [14]. Lastly, SAM encounters difficulties in video segmentation tasks due to the temporal continuity and dynamic features inherent in video data [15], which differ significantly from the requirements for static images. To address these limitations, SAM2 [16], an improved version of SAM, has been introduced. SAM2 is designed to better accommodate the specific needs of various segmentation tasks, offering more robust and accurate solutions for both image and video segmentation [11].

To gain a deeper understanding of SAM2’s role in image and video segmentation and provide a comprehensive perspective, we conducted a systematic review of relevant research [17], [18], [19], [20], [22]. Although some surveys summarize segmentation methods based on SAM or SAM2, these reviews often focus on specific domains or problems,

- Jiaxing Zhang is with the School of Software engineering, Sichuan University, Chengdu 610065, China. E-mail: 2022141420175@stu.scu.edu.cn.
- Hao Tang is with the School of Computer Science, Peking University, Beijing 100871, China. E-mail: haotang@pku.edu.cn

*Corresponding author: Hao Tang.

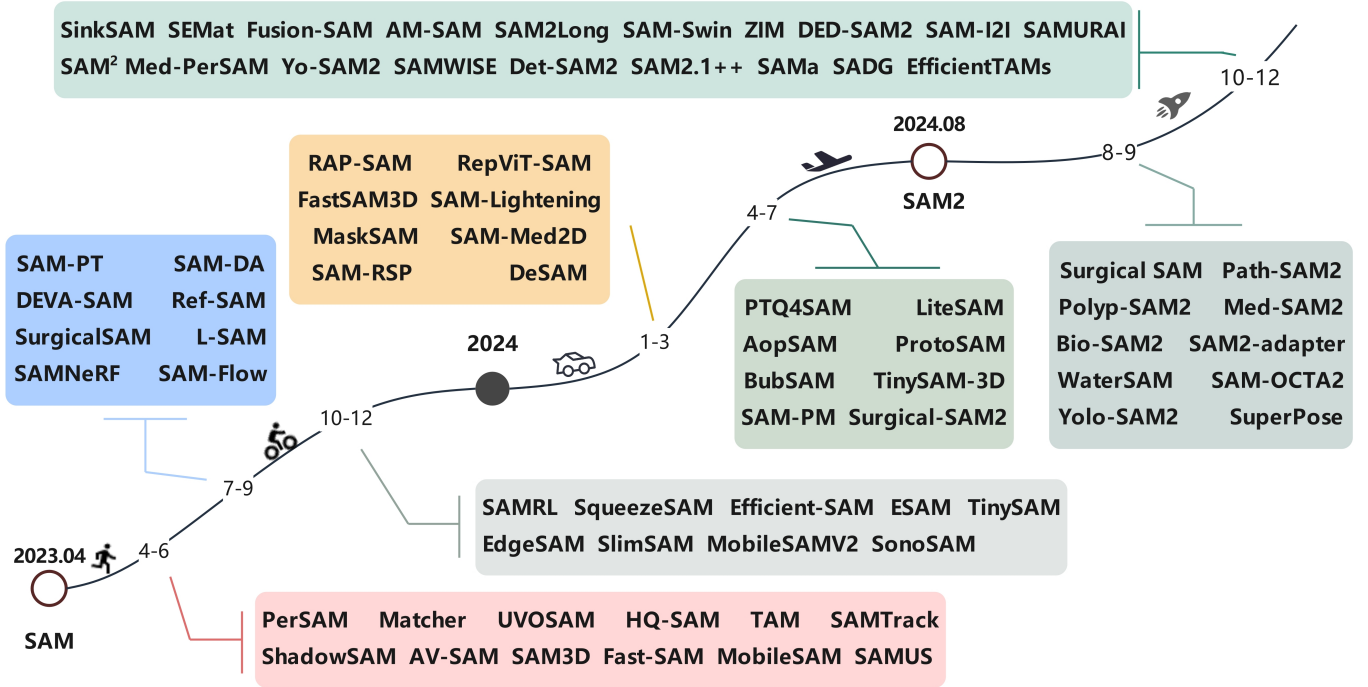


Fig. 1: This image illustrates the evolution and categorization of the SAM (Segment Anything Model)/SAM2 and its derivatives. Different colors and positions are used to clearly represent each model along the timeline. In addition to compiling various SAM/SAM2 variants in the field of segmentation, including tasks such as shadow detection and classification, we place particular emphasis on the progression of segmentation tasks.

overlooking the broader applications of SAM2 in both image and video segmentation (see Table 1). This review is the first to comprehensively evaluate SAM2’s performance, highlighting its effectiveness in segmentation tasks, while also examining its adaptability and limitations across different domains.

This study focuses on analyzing SAM2’s performance in image and video segmentation tasks across various fields. First, we provide a comprehensive overview of image segmentation, foundational model concepts and classifications, and the technical characteristics of SAM and SAM2. We also discuss the efforts to extend SAM/SAM2 into other domains. Next, we summarize recent research advancements and evaluate SAM2’s segmentation performance in two primary areas: video and static images. In analyzing its performance on natural images, we place particular emphasis on its application in the specialized field of medical imaging, as studies in other specialized fields remain limited. Finally, we summarize SAM2’s characteristics in image and video segmentation, discuss current technical challenges, and explore future development directions.

The main objective of this study is to evaluate SAM2’s performance in image and video segmentation tasks. Section 2 introduces the fundamental concepts of segmentation, covering the basics of image segmentation, the classification of foundational models, and a detailed comparison of SAM and SAM2, emphasizing their strengths and differences across tasks. Section 3 reviews the latest research and applications of SAM2 in image segmentation. We examine state-of-the-art networks, summarize SAM- and SAM2-based methods, collect datasets for natural and medical images, and discuss commonly used evaluation metrics to

establish a theoretical foundation for performance assessment. In Section 4, we shift focus to video segmentation tasks and evaluate SAM2’s performance in dynamic scenes. We classify recent video segmentation networks, compile relevant video datasets, and introduce evaluation metrics in this domain to provide a comprehensive analysis of SAM2’s capabilities. Finally, Section 5 summarizes SAM2’s characteristics in image and video segmentation, identifies the technical challenges it faces, and offers insights into future development directions. Through this study, our objective is to provide valuable information and actionable recommendations for the application and further optimization of SAM2 in real-world scenarios.

2 PRELIMINARIES

In this section, we provide a concise introduction to problem formulation, key topics, and concepts, aiming to enhance comprehension of our work.

2.1 Image Segmentation and Video Segmentation

Image segmentation has been a foundational problem in computer vision since the early days of the field. It can be defined as the task of classifying pixels with semantic labels (semantic segmentation), partitioning individual objects (instance segmentation), or addressing both tasks simultaneously (panoptic segmentation). Semantic segmentation [23], [24], [25] assigns each pixel to a predefined semantic class label. Instance segmentation [26], [27], [28] goes a step further by distinguishing between instances of the same class. Panoptic segmentation, introduced by [29],

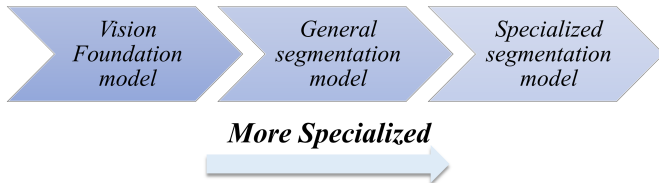


Fig. 2: this image illustrates the hierarchical structure of visual models, progressing from foundational visual models to general segmentation models, and then to specialized segmentation models, reflecting an increasing level of specialization to meet the needs of more specific visual tasks.

integrates semantic and instance segmentation to provide a comprehensive understanding of scenes. As the demand for more precise and user-friendly segmentation techniques has increased, **interactive segmentation** has emerged as a key approach in this domain. Interactive segmentation enables users to actively participate in the segmentation process by providing input and feedback, such as marking regions of interest or correcting errors. This interactive involvement aims to improve both the accuracy and efficiency of segmentation results. Unlike traditional semantic or instance segmentation methods, interactive segmentation empowers users to refine outputs dynamically, making it particularly effective in complex and ambiguous scenes.

Video segmentation is a crucial task in computer vision, aimed at classifying or segmenting each pixel in every frame of a video sequence into distinct objects and backgrounds [30]. It can be broadly categorized into two types: Video Object Segmentation (VOS) and Video Semantic Segmentation (VSS) [31]. VOS focuses on isolating specific objects in a video without requiring detailed semantic labels, whereas VSS assigns each pixel to predefined semantic categories (e.g., “person” or “car”) while ensuring label consistency across frames. In recent years, **zero-shot** and **few-shot** learning approaches have attracted significant attention in video segmentation. Zero-shot learning performs segmentation tasks without requiring any training samples, whereas few-shot learning enables effective model training using only a small number of labeled samples.

While image segmentation is well-suited for static scenarios with lower computational complexity, video segmentation involves processing multiple frames, making it computationally intensive. It is specifically designed for dynamic scenarios that require higher performance and advanced techniques to handle the added complexity.

2.2 Foundation Models

Foundation models (e.g., [32]) refer to machine learning models that perform well on specific tasks and are pre-trained on large-scale datasets. Their design aims to enhance the model’s generalizability and transferability, enabling it to perform well across various downstream tasks. As shown in Figure 2, the trend towards increasingly refined models is presented. The characteristics of foundation models can be summarized with three keywords: large-scale pre-training, generalizability, and transferability.

2.2.1 Vision Foundation Models

The Visual Foundation Model [33] is an advanced deep learning architecture designed to handle various visual tasks through a unified framework. These models are typically pre-trained on large-scale datasets to learn rich visual features, thereby enhancing their performance across multiple downstream tasks. The design of visual foundation models aims to achieve efficient feature extraction and multimodal understanding, enabling their application in fields such as image classification, object detection, image segmentation, and image generation. A notable example is CLIP [34], which uses contrastive learning to map images and text into the same feature space, allowing it to understand and generate textual descriptions related to visual content. Additionally, the Vision Transformer (ViT) [35], [36] effectively processes image data using self-attention mechanisms, adapting to various visual tasks. The emergence of these models has accelerated the rapid development of computer vision, providing strong support for practical applications.

2.2.2 General Segmentation Models

A general segmentation model is designed to handle a variety of objects and tasks within image segmentation, capable of addressing various types of image segmentation tasks through a unified framework. The most typical example is the Segment Anything Model [10], which is the first promptable general image segmentation model. SAM exemplifies the capabilities of foundation models, showcasing outstanding generalizability through pre-training on large-scale datasets and the ability to adapt to different domains via transfer learning. Consequently, this model shows extensive potential in applications such as medical imaging, autonomous driving, and robotic vision, providing fast and accurate segmentation results that enhance task efficiency and accuracy. Leveraging an efficient self-attention mechanism, SAM quickly responds to various scenarios, meeting modern applications’ demands for real-time processing.

Building on this, SAM2 [16] further enhances the model’s performance and flexibility. It introduces more complex feature extraction techniques and improved multimodal learning capabilities, allowing it to excel in handling complex backgrounds and diverse objects. Through optimized training strategies, SAM2 achieves high-quality segmentation with less annotated data, demonstrating greater adaptability and ease of integration with other systems. Additionally, SAM2 supports more detailed segmentation and higher resolutions, further improving precision and reliability in specific tasks. These enhancements make SAM2 more efficient in practical applications, capable of meeting the growing demands for real-time processing and high precision.

2.2.3 Comparison of Specialized Models and Foundation Models

From a definitional standpoint, specialized models possess in-depth expertise on specific topics, while foundation models encompass broader domain knowledge, whether within a single field or across multiple disciplines. Taking medical image segmentation as an example, **specialized foundational segmentation models** are often optimized for

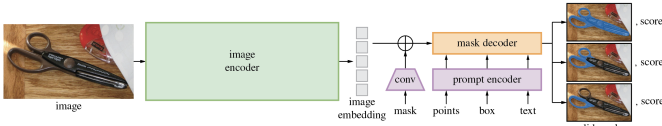


Fig. 3: Segment anything [10]

specific organs or tasks, thus providing higher accuracy and interpretability in relevant segmentation tasks. In contrast, **general segmentation models** serve as a multitasking and multimodal platform that can process multimodal images of various organs and diseases. Our goal is to leverage general segmentation models to achieve convenient segmentation functionality while reaching or even surpassing the precision levels of specialized segmentation models.

2.3 Evolution of Image Segmentation

2.3.1 SAM: Segment Anything

As shown in Figure 3, Segment anything [10], as the first foundational model proposed for promptable image segmentation, consists primarily of three main components: the Image Encoder, Mask Decoder, and Prompt Encoder.

Image encoder uses a MAE [37] pre-trained Vision Transformer (ViT) [36] minimally adapted to process high resolution inputs.

Prompt encoder is crafted to process diverse user inputs—such as points, boxes, or text—by incorporating positional encodings [38] to guide the segmentation process. It encodes these prompts into a feature space aligned with the image features generated by the image encoder, enabling seamless integration and effective guidance during segmentation.

Mask decoder utilizes a modified Transformer decoder block [39], followed by a dynamic mask prediction head, to generate segmentation masks by effectively combining image embeddings with prompt embeddings.

2.3.2 SAM2: Segment Anything in Images and Videos

As shown in Figure 4, Segment Anything Model 2 (SAM2) [16] is an advanced visual segmentation model that builds on its predecessor, SAM [10], by incorporating a transformer-based architecture combined with a streaming memory component. This enhancement allows SAM2 to support real-time video segmentation and object tracking, addressing the dynamic challenges posed by moving scenes. SAM2’s architecture is optimized for real-time video segmentation and object tracking, featuring several key components. The **Hierarchical Image Encoder** performs initial feature extraction, generating unconditioned tokens for each frame, and running once per interaction to provide frame representations. The **Memory Attention Module** leverages temporal context by conditioning current frame features on those from past frames, along with prior predictions and any new prompts, using efficient self- and cross-attention mechanisms [40].

To handle user input, the **Prompt Encoder**—identical to SAM’s—interprets prompts like clicks (positive or negative), bounding boxes, or masks to specify the object’s extent within a frame. The **Mask Decoder** then generates

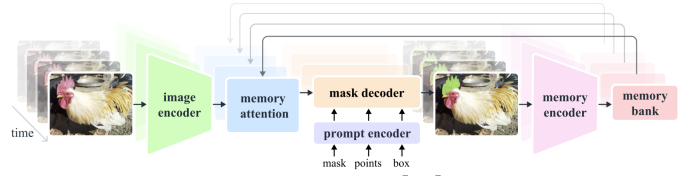


Fig. 4: SAM2 [16]

segmentation masks, maintaining the SAM’s approach for continuity. The **Memory Encoder** refines memory features by downsampling output masks and integrating them with unconditioned frame embeddings through lightweight convolutional layers. Lastly, the **Memory Bank** stores past predictions, enhancing accuracy and reducing the need for user input. Together, these components boost SAM2’s segmentation accuracy and efficiency, reducing interactions, and significantly speeding up image segmentation tasks. SAM-2 has demonstrated impressive zero-shot performance in various tasks that involve natural image and video segmentation.

2.3.3 Comparison between SAM and SAM2

There are significant differences between SAM and SAM2 in terms of applicable scope, architecture, and real-world application scenarios [11], [41]. In terms of **architecture**, SAM consists of a basic combination of an image encoder, mask decoder, and prompt encoder, while SAM2 builds on this foundation with the addition of a streaming memory component, which includes a hierarchical image encoder, memory attention module, and memory bank. These modules enable SAM2 to maintain consistency and accuracy across multiple frames. Regarding **prompting methods**, both SAM and SAM2’s prompt encoders support inputs such as points, boxes, and text, but SAM2 leverages memory from previous frames in multi-frame environments to reduce user input. For **application scenarios**, SAM is commonly used for single-frame segmentation tasks, such as object recognition, while SAM2 supports object tracking across video sequences, making it particularly suitable for scenarios requiring temporal continuity, such as video editing and dynamic object detection in autonomous driving. In terms of **applicable scope**, SAM primarily targets static image segmentation tasks, such as object segmentation in single-frame images, useful in areas like medical image analysis or satellite image segmentation. SAM2, on the other hand, extends further into video segmentation and object tracking, focusing on real-time processing in dynamic scenes, making it well suited for continuous-frame tasks such as autonomous driving and video surveillance.

3 SAM2 FOR IMAGE

Image segmentation divides the input image or video into multiple regions to distinguish different objects or structures. Accurate segmentation results help extract the regions or objects of interest and provide a foundation for subsequent analysis and processing, which is crucial for advanced computer vision tasks such as semantic understanding.

This subsection provides a comprehensive overview of image segmentation. We have compiled the current state-of-the-art models, particularly those based on SAM and

SAM2. In addition, we summarize commonly used datasets and evaluation metrics for assessing image segmentation methods.

3.1 Image Segmentation Networks

Table 2 presents a convenient reference for understanding the future of image segmentation in the field of deep learning by presenting segmentation methods from recent years.

Initially, early image segmentation methods relied on traditional machine learning techniques, typically using hand-crafted features for segmentation. With the advent of convolutional neural networks, image segmentation entered a new phase, where researchers began developing specialized segmentation models that achieved state-of-the-art performance on specific datasets. In recent years, the general-purpose segmentation model SAM has demonstrated significant superiority, providing more accurate and robust segmentation results in various scenarios. To further enhance segmentation precision and efficiency, SAM2 was introduced, offering faster processing times and more accurate segmentation, particularly in complex scenes and resource-constrained environments. SAM2 excels at handling large-scale datasets and real-time applications, driving significant advancements in the field of image segmentation. In the following subsections, we provide a detailed description of the characteristics and applications of these methods.

3.1.1 Specialized SOTA Models

Specialized *state-of-the-art* models are designed with specific tasks in mind. These models are typically optimized for particular datasets or applications, achieving high performance in controlled environments. By focusing on a narrow range of problems, specialized models can outperform general-purpose approaches in terms of accuracy and efficiency for specific segmentation tasks.

- nn-Unet [58] is an automated medical image segmentation method based on U-Net, capable of automatically optimizing the network structure and adapting to various medical image tasks.
- MedSegDiff [64], based on Diffusion Probabilistic Models (DPM), enhances medical image segmentation performance with Dynamic Conditional Encoding and Feature Frequency Parser, widely applied to different medical tasks.
- TransUnet [59] combines Transformers and U-Net, leveraging Transformers to capture global context, while U-Net enhances local details, improving medical image segmentation accuracy.
- iMOS [62] is a medical image segmentation model based on Diffusion Models, designed for dynamic object segmentation, achieving efficient tracking and segmentation with minimal annotations.
- UniverSeg [60] performs precise medical image segmentation without additional training, using the Cross-Block mechanism with a query image and a sample set, suitable for unseen tasks.
- FCFI [61] focuses on and collaboratively updates feedback and deep features, maximizing the use of feedback information in interactive segmentation to improve segmentation accuracy and efficiency.

- OnePrompt [65] combines single annotation and interactive segmentation methods, handling unseen tasks without training, demonstrating zero-shot capabilities in medical image segmentation.

These task-specific models are commonly used as baselines to evaluate the performance of general-purpose models. Since they are fine-tuned for specific tasks and provide high-accuracy segmentation results, they are often used as a standard to assess the effectiveness of new models. In comparative evaluations, general-purpose models must demonstrate performance comparable to or surpassing that of task-specific models to prove their effectiveness and robustness across diverse applications.

3.1.2 SAM-based Models

SAM-based models (Segment Anything Model) are general-purpose segmentation frameworks that provide a flexible and robust solution across a wide range of segmentation challenges. Unlike task-specific models, SAM is designed to handle diverse datasets, offering improved adaptability and accuracy in real-world applications. These models have set new benchmarks in the segmentation field by simplifying the task of segmenting complex scenes.

- MedSAM [12] adapts the Segment Anything Model (SAM) for medical image segmentation, using domain-specific prompts to enhance segmentation performance on medical tasks and improve generalization in medical images.
- SAM-Med2D [13] is a large-scale 2D medical image segmentation dataset that integrates diverse medical images and the corresponding masks, which helps the development of specialized segmentation models for medical applications.
- PerSAM [44] is a personalization method for SAM that enables task-specific segmentation with a single reference mask and image, adapting SAM without re-training and achieving personalized segmentation.
- SAM-Adapter [45] enhances SAM's performance on challenging downstream tasks by incorporating task-specific knowledge using simple adapters, significantly improving segmentation results for specialized tasks.
- SAM-MPA [49] is an extension of SAM for multi-modal medical image segmentation, improving performance by combining modality-specific information to adapt SAM's segmentation capabilities across different imaging techniques.
- IMIS-Net [46] designed for interactive medical image segmentation, utilizing dense mask generation through interactive inputs such as clicks, bounding boxes, and text prompts. It achieves superior accuracy and scalability in medical image segmentation tasks.
- EVF-SAM [51] combines visual and text prompts, enhancing SAM's performance in referring segmentation tasks through early visual-language fusion, reducing parameters, and achieving higher performance.

3.1.3 SAM2-based Models

SAM2-based models represent the next evolution of the SAM framework, offering enhanced performance in terms of both speed and segmentation precision. Using advanced techniques and optimized architectures, SAM2 is capable of

TABLE 2: Recent advancements in image-segmentation networks, categorizing them by their foundational architecture and highlighting their unique features and targeted applications, with a particular emphasis on the evolution and capabilities of SAM and SAM2-based methodologies.

Classification	Method	Year	Pub.	Backbone	Feature	Tasks
SAM-based	MedSAM [12]	2023	Nature	SAM backbone	Fine-tuned	universal MIS
	MobileSAM [42]	2023	RS	SAM backbone	Lightweight, Efficient	sVOS
	SAM-Aug [43]	2023	Arxiv	SAM backbone	Point Augmentation	iVOS
	SAM-Med2D [13]	2023	Arxiv	SAM backbone	Large-scale	universal MIS
	PerSAM [44]	2023	Arxiv	SAM backbone	personalization	Personalized imageSeg
	SAM-Adapter [45]	2023	ICCV	SAM backbone	Adaptability	downstream tasks
	IMIS-Net [46]	2024	BIBM	SAM backbone	pre-trained	interactive MIS
	Fusion-SAM [47]	2024	Arxiv	SAM backbone	multi-modal	autonomous driving
	Point-SAM [48]	2024	Arxiv	SAM backbone	Point-supervised	RSIS
	SAM-MPA [49]	2024	Arxiv	SAM backbone	K-centroid clustering	Few-shot
CAT-SAM [50]	2024	ECCV	SAM backbone	Efficient Adaptation	Zero-shot	
EVF-SAM [51]	2024	Arxiv	SAM backbone	multi-modal	universal IS	
SAM2-based	MedSAM2 [52]	2024	Arxiv	SAM2 backbone	OnePrompt Seg	universal 2D and 3D MIS
	Bio-SAM2 [53]	2024	Arxiv	SAM2 backbone	Enhanced Biomedical Model	universal MIS
	SAM-OCTA 2 [54]	2024	Arxiv	SAM2 backbone	Fine-tuned	Zero-shot
	DED-SAM [55]	2024	IEEE J-stars	SAM2 backbone	Change detection	RSIS
	SAM2-Adapter [56]	2024	Arxiv	SAM2 backbone	Broad adaptability	Downstream tasks
	PATH-SAM2 [57]	2024	Arxiv	SAM2 backbone	Fine-tuned	digital pathology
Others	nn-Unet [58]	2021	Nature	Unet	Automation, Generality	task-tailored
	TransUnet [59]	2021	Arxiv	Transformer, Unet	Hybrid architecture	task-tailored
	UniverSeg [60]	2023	ICCV	FCN	Zero-shot generalization	universal MIS
	FCFI [61]	2023	CVPR	ResNet-101	Feedback-Driven	interactive imageSeg
	iMOS [62]	2024	ISBI	XMem [63]	Minimal annotation	Few-shot
	MedSegDiff [64]	2024	MIDL	diffusion model	Conditional diffusion	task-tailored
	OnePrompt [65]	2024	CVPR	CNN/ ViT	Single prompt	interactive MIS, Zero-shot

achieving accurate segmentation in complex and resource-constrained environments. This model is particularly well-suited for large-scale datasets and real-time applications, further advancing the capabilities of image segmentation.

- MedSAM2 [52], the evolved version of MedSAM, designed to further enhance the segmentation of medical images. It offers improved accuracy and efficiency for medical image processing tasks, incorporating advanced techniques to handle complex anatomical structures more effectively.
- Bio-SAM2 [53], focuses on the segmentation of biological images, incorporating domain-specific knowledge to achieve precise and adaptive segmentation for various biological imaging modalities.
- SAM2-Adapter [56] is an adapter for SAM2 that integrates domain-specific knowledge and visual prompts, improving SAM2’s performance in challenging segmentation tasks in medical imaging.
- SAM-OCTA2 [54] is tailored for Optical Coherence Tomography Angiography (OCTA) images, SAM-OCTA 2 enhances the segmentation of vascular structures with specialized techniques for OCTA data.
- Path-SAM2 [57] designed for pathology images, utilizing advanced adaptations of SAM to accurately segment histopathological structures for medical diagnosis.

In addition to these variations, existing works have systematically summarized the performance of SAM2 in medical imaging. Sengupta et al. [11] compares the advancements of SAM2 relative to SAM in medical image

segmentation, Dong et al. [66] explores the performance of SAM2 on 3D images, Shen et al. [67] investigates SAM2’s performance in interactive segmentation, He et al. [68] evaluates SAM2’s performance in 3D CT image segmentation, with results being less than ideal, Xiong et al. [69] attempts to use SAM2 as an encoder for UNet, demonstrating its strong adaptability in image segmentation, Ma et al. [70] quickly adapts SAM2 to the medical domain through fine-tuning, Yamagishi et al. [71] evaluates SAM2’s zero-shot performance on the abdominal organ CT scan dataset, Yildiz et al. [72] adapts SAM2 for annotating 3D medical images and implements it through the 3D Slicer extension, supporting prompt-based annotation generation and propagation across volumes, Zhao et al. [73] focuses on the context dependence of SAM2. These evaluations have pushed the expansion of SAM2 across different domains.

3.2 Datasets

Next, we will specifically discuss widely used datasets for model training and evaluation, focusing on natural and medical scenes. In terms of natural scenes, there is already a wealth of research and datasets, so we will not go into further detail. However, in medical scenes, different datasets have varying requirements for models, so we will focus on this aspect.

3.2.1 Natural datasets

Natural scene datasets are widely used in computer vision research, supporting tasks such as object detection, segmentation, and scene understanding. These datasets covers var-

ious environments, from urban to natural settings, offering diverse data for model training. Specific dataset information is provided in Table 3, and we will now provide a detailed introduction below.

- **UnderWater** datasets focus on underwater segmentation, addressing challenges such as lighting, turbidity, and distortions. For example, TrashCan [74] collects data on underwater trash, while CoralVOS [76] focuses on segmenting dense coral images. NDD20 [75] covers both underwater and above-water dolphin imagery, aiming to segment marine life across environments.
- **Plants** datasets are used for segmentation and classification in botanical environments. PPDLS [77] focuses on tobacco leaves, while MSU-PID [78] tracks *Arabidopsis* plant growth. KOMATSUNA [79] captures images of Komatsuna leaves, all addressing the challenge of segmenting plants with diverse shapes, textures, and backgrounds.
- **Scene** category includes datasets for scene understanding, featuring a range of environments and contexts. ADE20K [84] covers diverse scenes and objects, for instance segmentation, while LVIS [85] focuses on long-tailed objects. COCO [81] is widely used for object detection and segmentation, with extensive image data. SUN [80] targets everyday scenes with semantic annotations, and Places [83] focus on scene objects in various settings. Cityscapes [82] is a specialist in urban street scenes, offering panoptic segmentation data. NDIS-Park [88], [89] and STREETS [86] provide instance-level segmentation for parking lots and street-level videos, respectively. iShape [87] emphasizes indoor shape and structure, and IBD [90] focuses on individual cell structure segmentation. These datasets help address the challenges of segmenting complex scenes in diverse environments.
- **Egocentric** datasets are captured from a first-person perspective, often using wearable cameras. VISOR [92] includes complex real-world scenes, while GTEA [91] and EgoHOS [93] focus on human-object interactions, tracking hand movements and object manipulation, with challenges such as occlusions and rapid motion.
- **Paintings** datasets focus on the segmentation of artistic works. DRAM [94] covers art paintings, while Seg-CLP [95] focuses on Chinese paintings. CLP [96] deals with Chinese landscape art, addressing the challenges in distinguishing artistic styles, brush strokes, and color variations in fine art.
- **Others:** The “Others” category includes datasets that don not fall into the above categories but are still valuable for specialized tasks in image segmentation. This may include niche applications such as industrial inspection, satellite imagery, or other unique domains that require specific segmentation techniques. These datasets present a diverse range of challenges, depending on the application, and require highly specialized models to achieve accurate segmentation results. **Others** encompasses diverse datasets for specialized image segmentation tasks. BBBC038v1 [98] targets biological nuclei segmentation, while DOORS [100] focuses on doorways and architectural elements. TimberSeg [101] is dedicated to operator-view timber log segmentation,

and OVIS [105] handles occlusion in videos. HyperSim [102] offers photorealistic indoor masks for segmentation, while WoodScape [99] focuses on surround fish-eye views. Plittersdorf [103] provides data for wildlife trap segmentation, and ZeroWaste-f [104] focuses on recycling waste. These datasets cater to unique, niche applications requiring specialized segmentation techniques across various domains.

3.2.2 Medical datasets

Medical scene datasets encompass various imaging modalities (such as CT, PET, MRI, ultrasound, etc.), different body parts (such as head and neck, chest, abdomen, etc.), and diverse dimensions (2D and 3D). To better understand and analyze these datasets, we classify them into single-organ and multi-organ categories. In the single-organ category, we further refine the classification based on specific body parts.

Table 4 categorizes the single-organ datasets into the following anatomical regions: Head and Neck, Thorax, Abdomen, Pelvis, Bone and Spine, Lesion, and Others. In addition, we have also collected large-scale datasets.

- **Head and Neck:** BraTs [106], a multimodal MRI dataset with 12,591 images, focused on brain tumor research; Hecktor [109], a PET/CT dataset with 489 images, primarily used for head and neck tumor analysis; Hippo [108] contains 260 MRI images focusing on hippocampal region segmentation; ANDI [107], a dataset with 68 MRI images for hippocampal segmentation; and TN3K [110], an ultrasound dataset with 3,493 images, focusing on thyroid nodule analysis.
- **Thorax:** Breast-US [113], a breast ultrasound dataset comprising 630 images; Chest-Xray [111], which includes 704 X-ray images for chest X-ray analysis; Covid19 [112], containing 11,956 X-ray images, primarily used for lung tissue analysis; ACDC [117], a dataset with 1,808 MRI and CMR images, focused on cardiac imaging; and CMR T1-Map [117], a myocardial imaging dataset with 50 CMR images. LA [115], a Left Atrium segmentation dataset utilizing LGE-MRI, with 154 3D images; CIR [116], a lung nodule detection dataset from MICCAI, consisting of 956 3D CT images; and BUID [114], a breast tumor detection dataset based on ultrasound, containing 780 images, 529 of which are annotated in 2D.
- **Abdomen:** Kidney-US [120], which contains 4,586 ultrasound images for kidney analysis in CT2US tasks; LiTs [121], a dataset of 5,501 CT images aimed at liver tumor analysis; Kvasir [119], featuring 1,000 endoscopic images designed for colon polyp detection; and **Pancreas** [118], a dataset with 285 CT images dedicated to pancreatic tissue analysis.
- **Pelvis:** Prostate [122], a prostate segmentation dataset with 79 3D MRI images; MMOTU [123], which contains 1,469 ultrasound images for ovarian tumor detection; and OAI-ZIB [124], a knee MR dataset with 488 3D MRI images.
- **Bone and Spine:** Spine-MRI [125], a dataset designed for spinal cord gray matter detection with 551 3D MRI images; VerSe [127], a vertebrae segmentation dataset comprising 374 3D CT images and 4,505 masks; and

TABLE 3: Natural image datasets, detailing categories, sizes, annotations, and publication sources, aiding dataset selection for computer vision tasks, especially image segmentation.

Category	Dataset	Description	# masks type	# images sampled	# masks sampled	Pub.
UnderWater	TrashCan [74]	Underwater trash	Instance	5936	9540	Arxiv2020
	NDD20 [75]	Above/underwater dolphin	Instance	4402	6100	Arxiv2020
	CoralVOS [76]	Dense coral	Panoptic	60456	60456	Arxiv2023
Plants	PPDLS [77]	Tobacco leaves	Instance	182	2347	PRL2016
	MSU-PID [78]	Arabidopsis growth	Instance	900	900	MVA2016
	KOMATSUNA [79]	Komatsuna leaves	Instance	576	576	ICCV2017
Scene	SUN [80]	everyday scenes	Semantic	130519	-	CVPR2010
	COCO [81]	Object detection, segmentation	Instance	330K	2.5M	ECCV2014
	Cityscapes [82]	Urban street scene	Panoptic	293	9973	CVPR2016
	Places [83]	Scene object, diverse settings	Semantic	10624928	7076580	TPAMI2017
	ADE20K [84]	range of scenes and objects	Instance	302	10128	IJCV2019
	LVIS [85]	Long-tailed object	Instance	945	9642	CVPR2019
	STREETS [86]	Street-level video	Instance	819	9854	NIPS2019
	iShape [87]	Shape and structure, indoor	Instance	754	9742	Arxiv2021
	NDISPark [88], [89]	parking lot footage	Instance	111	2577	IJCV2021
	IBD [90]	individual cell structures	Instance	467	11953	IEEE IGRS 2022
Egocentric	GTEA [91]	human-object interactions	Instance	652	12.8	CVPR2015
	VISOR [92]	complex real-world scenes	Instance	1864	10141	NIPS2022
	EgoHOS [93]	Ego-centric hand-object	Instance	2970	9961	ECCV2022
Paintings	DRAM [94]	Art paintings	Semantic	718	1179	CGF2022
	SegCLP [95]	Chinese paintings	Semantic	709	709	DSP2024
	CLP [96]	Chinese landscape paintings	Semantic	2207	-	NCA2024
Zero-shot	SA-1B [10]	dense masks	Semantic	11M	1.1B	ICCV2023
	MicroMat-3K [97]	Micro-level matte labels	Semantic	3000	-	Arxiv2024
Others	BBBC038v1 [98]	Biological nuclei	Instance	227	10506	Natures2019
	WoodScape [99]	Surround fisheye	Instance	107	10266	NIPS2019
	DOORS [100]	doorways, architectural elements	Instance	10000	10000	Zenodo2022
	TimberSeg [101]	Operator-view timber logs	Instance	220	2487	IROS2022
	Hypersim [102]	Photorealistic indoor masks	Instance	338	9445	ICCV2021
	Plittersdorf [103]	Wildlife traps	Instance	187	546	Sensors2022
	ZeroWaste-f [104]	Recycling waste	Instance	2947	6155	CVPR2022
	OVIS [105]	Occlusion in videos	Instance	2044	10011	ICCV2023

SpineSeg [126], a spine MR imaging dataset containing 215 3D images.

- **Lesion:** Fdg-PET [129], a tumor lesion dataset with 1,015 3D PET/CT images; ISIC [128], which contains 2,750 2D images for skin lesion detection; and ISLES [130], [131], a dataset for stroke lesion detection with 400 3D MRI images.
- **Large Scale:** IMed-361M [46], a large-scale dataset with 6.4 million images across 14 modalities, supporting zero-shot segmentation; SA-1B [10], a universal segmentation dataset with 11 million images spanning 2D modalities; COSMOS [132], an 18-modality dataset with 1.05 million images, designed for zero-shot segmentation; onePrompt [65], which contains approximately 3,000 2D and 3D images supporting IMIS; SA-Med2D [13], a 2D universal segmentation dataset with 4.6 million images across 10 modalities; MedSAM [12], a universal segmentation dataset with 1.57 million images across 10 modalities; and OmniMedVQA [133], a medical question-answering dataset encompassing 12 modalities and 118,010 images.
- **Others:** HC [135], a dataset of 999 2D ultrasound images for fetal head circumference measurement; OCTA-500 [137], which includes 500 3D images for retinal vessel detection; EBHI [138], a dataset with 4,456 2D H&E stained histopathological images; CRAG [136], which contains 213 2D H&E stained adenocarcinoma slides; GlaS [134], a dataset with 165 2D H&E stained images for colorectal adenocarcinoma detection; and

FUSC [139], a foot ulcer detection dataset with 1,210 2D RGB images.

Table 5 compiles multi-organ datasets that encompass multiple body organs, modalities, and dimensions.

- The MSD dataset [108] provides a comprehensive collection for multi-organ segmentation with 7 modalities, including both 2D and 3D images. It covers a wide range of organs such as Brain Tumour, Heart, Liver, Hippocampus, and Spleen, offering a valuable benchmark for evaluating and developing segmentation algorithms across multiple organ types and imaging modalities.
- CT-organ [141] is a 3D CT dataset focusing on abdominal organs, including liver, bladder, lungs, kidneys, and bones. This dataset plays a crucial role in advancing CT-based segmentation techniques, particularly for abdominal imaging, and serves as a resource for improving segmentation performance in clinical and research settings.
- BTCV [142] is a dataset designed for the segmentation of body tumors and various organs. It includes challenging cases of diverse organ structures and tumors, providing a platform for evaluating segmentation methods on real-world medical images, especially in the context of tumor detection and organ delineation in the abdomen and thoracic regions.
- AbdomenCT-1K [143] includes 3D CT images from multiple medical centers, offering a large-scale resource for abdominal organ segmentation. With a wide variety

TABLE 4: Single-organ datasets, including the dataset name, year of publication, related papers, imaging modalities, the number of images and masks, data dimensions, and descriptive annotations.

Anatomical	Dataset	Year	Pub.	Modality	Images	Masks	Dimension	Descr.
Head and Neck	BraTs [106]	2014	TMI	MRI	-	12591	3D	Multimodal Brain Tumor
	ANDI [107]	2015	-	MRI	68	-	3D	Hippocampal segmentation
	Hippo [108]	2019	Arxiv	MRI	260	-	3D	Hippocampus
	Hecktor [109]	2022	MIA	PET/CT	489	489	3D	Head and neck
	TN3K [110]	2023	CBM	Ultrasound	3493	-	2D	thyroid nodules
Thorax	Chest-Xray [111]	2014	QIMS	X-ray	-	704	2D	Chest X-ray
	Covid19 [112]	2019	CBM	X-ray	11956	-	2D	Pulmonary tissues
	Breast-US [113]	2020	SCI	Ultrasound	-	630	2D	Breast Ultrasound
	BUID [114]	2020	dib	Ultrasound	780	529	2D	Breast tumor
	LA [115]	2021	MIA	LGE-MRI	154	-	3D	Left atrium
	CIR [116]	2022	MICCAI	CT	956	-	3D	Lung nodule
	ACDC [117]	2024	Arxiv	MRI, CMR	1808	-	2D	Cardiac Image
	CMR T1-Map [117]	2024	Arxiv	CMR	50	-	2D	Myocardium Image
Abdomen	Pancreas [118]	2018	ASO	CT	285	-	3D	Pancreatic parenchyma
	Kvasir [119]	2020	MMM	Colonoscopy	1000	-	2D	Polyps
	Kidney-US [120]	2022	Ultrasonics	Ultrasound	-	4586	2D	CT2US for Kidney
	LiTs [121]	2023	MIA	CT	-	5501	3D	Liver tumor
Pelvis	Prostate [122]	2020	TMI	MRI	79	-	3D	Prostate segmentation
	MMOTU [123]	2022	Arxiv	Ultrasound	-	1469	2D	Ovarian Tumor
	OAI-ZIB [124]	2024	Arxiv	MRI	488	-	3D	Knee MR volumes
Bone and spine	Spine-MRI [125]	2017	Neuroimage	MRI	-	551	3D	Spinal Cord Grey Matter
	SpineSeg [126]	2020	TMI	MR	215	-	3D	SpineMR
	VerSe [127]	2021	MIA	CT	374	4505	3D	Vertebrae Segmentation
Lesion	ISIC [128]	2017	ISBI	Dermoscopy	2750	-	2D	Skin Lesion
	fdg-PET [129]	2022	Nature	PET/CT	-	1015	3D	Annotated tumor lesions
	ISLES [130], [131]	2022	SCI	MRI	400	-	3D	Stroke Lesion
Large Scale	SA-1B [10]	2023	ICCV	-	11M	1.1B	2D	Universal segmentation
	SA-Med2D [13]	2023	Arxiv	10 modalities	4.6M	19.7M	2D	IMIS, Zero-shot and so on
	MedSAM [12]	2023	Nature	10 modalities	1570263	1570263	2D, 3D	Universal segmentation
	COSMOS [132]	2024	MIA	18 modalities	1050K	6033K	2D	IMIS, Zero-shot and so on
	onePrompt [65]	2024	CVPR	-	-	3000	2D, 3D	IMIS
	OmniMedVQA [133]	2024	CVPR	12 modalities	118010	-	2D, 3D	20 anatomical regions
	IMed-361M [46]	2024	BIBM	14 modalities	6.4M	361M	2D, 3D	IMIS, Zero-shot
Other	GlaS [134]	2017	MIA	H&E stained images	165	-	2D	Colorectal Adenocarcinoma
	HC [135]	2018	PIoS	Ultrasound	999	-	2D	Fetal head circumference
	CRAG [136]	2019	MIA	H&E stained images	213	-	2D	Adenocarcinoma Slides
	OCTA-500 [137]	2020	MIA	OCT/OCTA	500	-	3D	Retinal vessels
	EBHI [138]	2023	FIM.	H&E stained images	4456	-	2D	Histopathological Images
	FUSC [139]	2024	MDPI	RGB	1210	-	2D	Foot ulcer

of images from different scanners, it provides an opportunity to test and refine segmentation methods that generalize across clinical settings, making it a critical tool for training deep learning models.

- CHAOS [144] consists of both 2D and 3D CT/MRI images focusing on abdominal organs, including liver, kidneys, and spleen. The dataset was specifically designed for segmentation algorithm development, providing ground truth annotations and diverse examples that facilitate the training and evaluation of models for abdominal organ segmentation in both CT and MRI modalities.
- Flare [145] offers 3D CT images of 13 abdominal organs, such as liver, kidneys, spleen, and intestines. The dataset is intended to support research in the segmenta-

tion of abdominal organs, with its focus on CT images helping to advance the development of segmentation techniques that can handle multiple organ types in a single scan.

- AMOS [146] is a 3D CT and MRI dataset containing images of 15 abdominal organs. This dataset supports multi-organ segmentation research, enabling the development of algorithms that can segment multiple organs simultaneously. It is particularly valuable for testing deep learning models in the complex task of segmenting multiple structures within the abdomen using both CT and MRI scans.
- TotalSegmentatorV2-CT [147] provides 3D CT and MRI images for whole-body organ segmentation. This dataset focuses on segmenting all major organs in the

TABLE 5: Collection of multi-organ datasets, detailing publication year, source, imaging modality, dimensionality, and the specific anatomical regions covered.

Dataset	Year	Pub.	Modality	Dimension	Anatomical
Dense-Vnet [140]	2018	TMI	CT, MRI	3D	pancreas, gastrointestinal tract (esophagus, stomach, duodenum), liver, spleen, left kidney, gallbladder
MSD [108]	2019	Arxiv	7 modalities	2D, 3D	BrainTumour, Heart, Liver, Hippocampus, Prostate, Lung, Pancreas, HepaticVessel, Colon, Spleen
CT-organ [141]	2019	TCIA	CT	3D	Liver, bladder, lungs, kidney, and bone
BTCV [142]	2020	TMI	CT	3D	Abdomen, Cervix, Brain, Heart, Canine Leg
AbdomenCT-1K [143]	2020	TPAMI	CT	3D	Multi-center Abdominal Organ: Liver, kidney, spleen, and pancreas.
CHAOS [144]	2021	MIA	CT, MRI	2D, 3D	Liver, kidney(s), spleen
Flare [145]	2022	Arxiv	CT	3D	Abdominal diseases: liver kidney, spleen, pancreatic, stomach sarcomas, colon ovarian, and bladder.
AMOS [146]	2022	NIPS	CT, MRI	3D	Spleen, right kidney, left kidney, gallbladder, esophagus, liver, stomach, aorta, inferior vena cava, pancreas, right adrenal gland, left adrenal gland, duodenum, bladder, prostate/uterus.
TotalSegmentatorV2-CT [147]	2023	RAI	CT, MRI	3D	27 organs, 59 bones, 10 muscles, 8 vessels.

human body and is designed to aid in the development of full-body segmentation algorithms, providing a valuable resource for researchers working on multi-organ segmentation in both CT and MRI modalities.

- Dense-Vnet [140] includes 3D CT and MRI images and focuses on abdominal organs such as the pancreas, liver, spleen, and gastrointestinal structures. The dataset supports research into dense organ segmentation techniques, providing a rich source of images for testing models that aim to segment complex anatomical structures in the abdominal region.

3.3 Evaluate Metrics

To effectively measure the performance and effectiveness of segmentation algorithms, evaluation metrics are crucial. These metrics not only help us verify whether the segmentation results meet expectations, but also provide objective standards for comparing the performance of different algorithms and models. In image segmentation tasks, the evaluation primarily focuses on two aspects: first, the **accuracy of the segmentation results**, i.e., whether the segmentation can accurately capture the target region, especially when the target’s shape is complex or there is overlap; and second, the **robustness of the model**, i.e., how well the model can adapt to different input conditions, such as changes in lighting, occlusions, and other factors. By considering these two factors comprehensively, we can fully assess the model’s practical performance and provide guidance for subsequent optimization.

3.3.1 Intersection over Union (IoU)

IoU is a metric used to measure the overlap between the predicted segmentation region and the ground truth region. It evaluates the accuracy of the segmentation by calculating the ratio of the intersection to the union of the predicted and true regions. A higher IoU indicates better segmentation accuracy.

$$\text{IoU} = \frac{|A \cap B|}{|A \cup B|}, \quad (1)$$

A is the predicted segmentation region, B is the ground truth region, $|A \cap B|$ is the area of intersection between the predicted and ground truth regions, $|A \cup B|$ is the area of union between the predicted and ground truth regions.

3.3.2 Dice Similarity Coefficient (Dice)

The Dice coefficient is another widely used metric similar to IoU, but mathematically different. It is particularly useful for assessing similarity between two sets, especially when the target region is small or irregular, as is common in medical image segmentation.

$$\text{Dice} = \frac{2 \cdot |A \cap B|}{|A| + |B|}, \quad (2)$$

The elements in (2) are the same as in the IoU formula.

3.3.3 Mean Intersection over Union (mIoU)

mIoU is the average IoU across all classes in a multi-class segmentation task. In multi-class problems, we compute the IoU for each class and then average them. mIoU provides a comprehensive measure of performance across all classes in a segmentation task.

$$\text{mIoU} = \frac{1}{N} \sum_{i=1}^N \frac{|A_i \cap B_i|}{|A_i \cup B_i|}, \quad (3)$$

N is the total number of classes, A_i and B_i are the predicted and ground truth regions for class i , $|A_i \cap B_i|$ and $|A_i \cup B_i|$ are the intersection and union areas for class i .

3.3.4 Pixel Accuracy (PA)

Pixel Accuracy is the simplest segmentation metric, which measures the proportion of correctly predicted pixels over the total number of pixels. PA can be used to evaluate the overall performance of the model, but may not reflect true performance in cases of class imbalance.

$$\text{PA} = \frac{1}{N} \sum_{i=1}^N 1(y_i = \hat{y}_i). \quad (4)$$

y_i is the ground truth value of the i -th pixel, \hat{y}_i is the predicted value of the i -th pixel, 1 is the indicator function, which is 1 if $y_i = \hat{y}_i$ (the prediction is correct), and 0 otherwise, N is the total number of pixels.

4 SAM2 FOR VIDEO

In this section, we will summarize the video segmentation architectures based on SAM and SAM2, and compare them with other state-of-the-art architectures. In addition, we will introduce relevant video segmentation datasets and provide commonly used evaluation metrics, along with an analysis of segmentation performance.

4.1 Video Segmentation Networks

From cutting-edge model architectures to the continuous expansion of application scenarios, video segmentation technology has demonstrated strong potential for handling complex temporal data and long-duration video segmentation tasks. Traditional video segmentation tasks are typically classified into video object segmentation (VOS), video semantic segmentation (VSS), and video instance segmentation (VIS).

With the emergence of general-purpose models, the concepts of zero-shot and few-shot segmentation have introduced new directions for video segmentation. In response to these complex video segmentation tasks, models based on various architectures, such as STCN, SegGPT, and DeAOT, have successfully addressed challenges including sVOS and iVOS by using advanced mechanisms and algorithms. Meanwhile, SAM2 and its derivative versions have made significant progress in integrating interactive segmentation, memory tracking, and few-shot learning techniques. In the following, we will provide a detailed introduction from three perspectives in Table 6: **state-of-the-art techniques**, **SAM-based models**, and **SAM2-based models**, followed by an in-depth analysis.

4.1.1 State of the Arts

The state-of-the-art models in video segmentation have significantly improved the ability to handle dynamic changes and long-duration video data by leveraging innovative deep learning technologies and architectures. Next, we will dive into the core features of these cutting-edge models and their notable contributions to video segmentation tasks.

- STCN [148] utilizes a ResNet-50 architecture and diverse voting across multiple frames to enhance video object segmentation. By integrating spatio-temporal information, STCN captures the dynamic changes and spatial relationships of objects, making it well suited for complex tasks like sVOS and iVOS, where objects undergo temporal and spatial variations.
- SegGPT [149] employs Vision Transformer (ViT) and Mask Prompting to handle complex objects in video segmentation. The ViT captures long-range dependencies across frames, while Mask Prompting improves segmentation accuracy, making SegGPT particularly effective in tasks like video object segmentation and instance segmentation, where precise segmentation is crucial.

- DeAOT [150] introduces decoupled propagation mechanisms, which enhance flexibility in handling dynamic target movement and scene changes. This mechanism improves object tracking accuracy, making DeAOT especially suitable for long-duration video segmentation tasks like iVOS and sVOS, where complex object motion must be tracked over time.
- RDE [151] enhances segmentation accuracy with region-based dynamic encoding, combining local and global contextual information to solve issues like occlusions and object interactions. RDE is robust in long-duration video segmentation tasks and performs efficiently, especially in real-time applications, where quick response and accuracy are critical.
- XMem [63] leverages memory consolidation techniques to improve long-term object tracking. By storing and updating target representations across frames, XMem ensures consistent tracking even with occlusions or appearance changes. This makes XMem ideal for long video sequences, particularly in tasks such as sVOS and iVOS that require identity maintenance over time.
- DEVA [153] uses the Mask2FormerR50 architecture for few-shot decoupled segmentation, enhancing generalization to new object categories with limited labeled data. This few-shot learning capability makes DEVA highly effective for tasks with sparse data, excelling in video object segmentation where only a small number of samples are available for training.
- DDMemory [154] employs dynamic memory banks to handle long-duration video object segmentation, storing, and updating target representations across multiple frames. This method improves segmentation precision, making it ideal for addressing challenges such as occlusion and motion blur in long-term video segmentation tasks.
- Cutie [155] optimizes video object segmentation using a lightweight, object-level memory architecture. This design balances computational efficiency and segmentation performance, making it well suited for real-time applications, particularly in resource-constrained environments where performance and efficiency are crucial for video segmentation tasks.
- LiVOS [156] adopts a lightweight memory architecture to optimize video object segmentation, maintaining both segmentation accuracy and computational efficiency. This model is particularly effective for long-duration video segmentation, ensuring high-precision target identification and continuous tracking, even as the target changes over time.

4.1.2 SAM-based Models

This class of models based on the SAM architecture represents the latest advancements in video segmentation, aiming to enhance performance in interactive segmentation, memory tracking, and few-shot learning tasks. SAM and its derivative models exhibit excellent performance in handling dynamic video scenes and long temporal sequences by incorporating innovations such as spatio-temporal memory and decoupled propagation mechanisms. Next, we will provide a detailed overview of how these models improve

TABLE 6: Video segmentation networks, categorizing them by their methodological approaches, publication years, backbone architectures, distinctive features, and the tasks they address, including state-of-the-art, SAM-based and SAM2-based methods.

Classification	Method	Year	Pub.	Backbone	Feature	Tasks
State of the Arts	STCN [148]	2021	NIPS	ResNet-50	Diversified Voting	sVOS
	SegGPT [149]	2021	ICCV	Vision Transformer	Mask Prompting	sVOS, iVOS, Zero-shot
	DeAOT [150]	2022	NIPS	Vision Transformer	Decoupled Propagation	sVOS
	RDE [151]	2022	CVPR	STM [152]	Self-correction	sVOS
	XMemo [63]	2022	ECCV	ResNet-50	Memory consolidation	sVOS
	DEVA [153]	2023	ICCV	Mask2FormerR50	Decoupled segmentation	Few-shot
	DDMemory [154]	2023	ICCV	ResNet	Dynamicmemory banks	LVOS
	Cutie [155]	2024	CVPR	ResNet-50/Res-net 18	Object-level memory	sVOS, LVOS
LiVOS [156]	2024	Arxiv	ResNet-50	Lightweight memory	sVOS	
SAM-based	SAM [10]	2023	ICCV	Vision Transformer	Universal Interactive Segmentation	sVOS, iVOS, Zero-shot
	DEVA-SAM [153]	2023	ICCV	SAM backbone	Decoupled Propagation	few-shot
	SAM-PT [157]	2023	Arxiv	SAM backbone	Point Propagation	iVOS, Zero-shot
	SurgicalSAM [158]	2023	AAAI	SAM backbone	Prototype-tuning	Zero-shot
	MemSAM [159]	2024	CVPR	MedSAM [12] backbone	Spatiotemporal Memory	sVOS
	VideoSAM [15]	2024	Arxiv	SAM backbone	Memory Tracking	sVOS
	SAM-PD [160]	2024	Arxiv	SAM backbone	Prompt Denoising	sVOS, iVOS
	RAP-SAM [161]	2024	Arxiv	SAM backbone	Real-time All-purpose	VSS, VIS, VPS, iVOS
SAM2-based	SAM2 [16]	2024	Arxiv	Vision Transformer	Universal	sVOS, iVOS, Zero-shot
	Yolo-SAM2 [162]	2024	Arxiv	YOLO v8 + SAM2	Bounding box-based	Zero-shot
	SurgicalSAM2 [163]	2024	Arxiv	SAM2 backbone	Efficient Frame Pruning	Zero-shot(Real time)
	PolypSAM2 [164]	2024	Arxiv	SAM2 backbone	different prompts	Zero-shot
	SAMWISE [165]	2024	Arxiv	SAM2 backbone	Multimodal Temporal	RVOS
	Det-SAM2 [166]	2024	Arxiv	SAM2 backbone	Pipeline	LVOS
	SAMURAI [167]	2024	Arxiv	SAM2 backbone	Robust	Zero-shot
	SAM2Long [168]	2024	Arxiv	SAM2 backbone	Pathway-optimization	sVOS, iVOS, Zero-shot

the accuracy and efficiency of video object segmentation through various techniques.

- SAM [10] is a versatile interactive segmentation model based on Vision Transformer (ViT), capable of handling sVOS, iVOS, and zero-shot segmentation without labeled data. It captures long-range dependencies, making it ideal for dynamic segmentation tasks.
- MemSAM [159] extends SAM with spatio-temporal memory, improving object tracking across frames. This enhancement aids in long-duration video segmentation, particularly for sVOS and iVOS tasks, by retaining and updating object representations.
- DEVA-SAM [153] introduces decoupled propagation mechanisms, which allow SAM to handle complex scenes with significant object changes. This improves flexibility and robustness for long-duration video segmentation tasks.
- VideoSAM [15] enhances video segmentation by focusing on dynamic memory tracking. It ensures accurate segmentation across frames, even in challenging scenarios like occlusions, by maintaining object identities over time.
- SAM-PT [157] improves SAM’s segmentation by using point propagation, leveraging sparse point annotations to refine object boundaries. This technique enhances accuracy in tasks like object instance and video object segmentation, where precision is crucial.
- SAM-PD [160] enhances segmentation by reducing noise in prompts. This approach improves accuracy in

ambiguous or noisy tasks, such as zero-shot segmentation and complex video sequences, ensuring focus on relevant features.

- RAP-SAM [161] is a real-time, versatile video segmentation model. It efficiently handles various challenges, from object tracking to scene understanding, suitable for interactive and live video analysis.
- SurgicalSAM [158] improves segmentation by combining multimodal temporal modeling with prototype tuning. This allows adaptation to unseen categories, making it effective for medical imaging tasks, particularly in surgery, where precise segmentation is critical.

4.1.3 SAM2-based Models

The SAM2-based models represent a significant advancement in the field of real-time video segmentation, leveraging the improved SAM2 architecture to address a variety of challenges. These models combine powerful techniques, such as efficient frame pruning, multimodal temporal modeling, and pathway optimization, to enhance segmentation accuracy and speed. Designed for applications that require real-time processing and adaptability, SAM2-based models excel in tasks like zero-shot segmentation, dynamic object tracking, and long-duration video analysis. In the following, we explore the key contributions of these models, highlighting their capabilities and applications in different domains.

- Yolo-SAM2 [162] integrates YOLO v8 and SAM2, focusing on enhancing object segmentation through bounding boxes. It achieves faster, accurate zero-shot seg-

mentation, especially in real-time scenarios. Leveraging YOLO's detection and SAM2's segmentation, it addresses challenges in dynamic environments, offering a robust solution for tasks with limited or no labeled data.

- SurgicalSAM2 [163] improves the real-time segmentation performance of SurgicalSAM by utilizing efficient frame pruning techniques. This enables faster processing of video frames, making it suitable for live-streaming scenarios. Its precision and speed make it ideal for high-stakes applications like surgery and medical imaging, ensuring accurate results with minimal computational resources.
- PolypSAM2 [164] examines SAM2's performance in polyp segmentation under various prompt settings, analyzing its strengths and limitations across datasets. The study evaluates segmentation accuracy, computational efficiency, and adaptability under different conditions, providing insights into the model's effectiveness in medical imaging tasks requiring high precision and reliability.
- SAMWISE [165] introduces a novel real-time video segmentation method combining multimodal temporal modeling and prototype tuning. It adapts to new object categories and complex scenes without retraining, excelling in zero-shot segmentation tasks. Its efficiency and accuracy make it ideal for medical diagnostics and autonomous vehicles, where rapid adaptation to new data is critical.
- Det-SAM2 [166]'s strengths lie in its automated object prompt generation and resource efficiency management, making it particularly suitable for long-duration video segmentation tasks requiring efficient inference.
- SAMURAI [167] is an enhanced version of SAM2 designed for visual object tracking. By integrating temporal motion cues and motion-aware memory selection, it achieves robust, real-time tracking with accurate mask selection, excelling in zero-shot tasks without fine-tuning.
- SAM2 [16] builds upon the original SAM model, offering enhanced efficiency and accuracy for real-time segmentation tasks. Powered by the Vision Transformer, SAM2 excels in dynamic video scenarios and extended tasks, delivering robust zero-shot capabilities for sVOS, iVOS, and applications with limited data. Its zero-shot inference demonstrates outstanding performance and resilience in surgical video segmentation [169].
- SAM2Long [168] optimizes SAM2 for long video segmentation using pathway strategies, maintaining accuracy over extended sequences. It handles longer temporal dependencies, ideal for video surveillance, environmental monitoring, and autonomous driving, requiring continuous object tracking.

4.2 Video Datasets

Table 7 summarizes several important video segmentation datasets that have been developed for various segmentation tasks, including video object segmentation, motion tracking, and complex scene analysis. These datasets provide valuable resources for training and evaluating video segmentation models that address various real-world challenges.

Each dataset varies in terms of the number of videos, object categories, annotations, and tasks, making them highly valuable for different research applications such as multi-object tracking, object detection, and real-time video segmentation. In the following, we briefly describe the key datasets and their respective characteristics and target tasks.

- SegTrack [170] is a small video segmentation dataset containing only 6 short videos with limited object categories, making it suitable for single-object segmentation tasks. SegTrack-v2 [171] expands on this, featuring 14 videos to support multi-object segmentation tasks and improving annotation accuracy, serving as a key resource for early multi-object tracking research.
- YouTube-Objects [172] includes 126 videos focusing on single-object segmentation, making it ideal for learning simple object segmentation from real-world scenarios. FBMS-59 [173] consists of 59 videos and 13,860 frames, covering 16 target categories, and is designed for evaluating multi-object segmentation. Jump-cut [174] contains 22 videos emphasizing clip-based segmentation tasks, making it a high-quality resource for analyzing dynamic objects.
- DAVIS16 [30] and DAVIS17 [175] are key video segmentation datasets. DAVIS16 focuses on single-object segmentation, while DAVIS17 extends to multi-object segmentation with 90 videos and 13,543 frames. The dataset is known for high-quality annotations and complex scenes, providing a solid benchmark for video object segmentation tasks.
- EndoVis17 [176]: A small dataset of 8 videos (255 frames each) for surgical instrument segmentation, with ground truth segmentation masks for each frame. EndoVis18 [177]: Includes 19 sequences for surgical image segmentation, with 15 for training and 4 for testing. Each sequence contains 300 frames with complex annotations of anatomical structures and surgical tools.
- CAMUS dataset [179] includes data from 500 patients, with 450 used for training. It provides 900 echocardiography sequences from GE Vivid E95 scanners, featuring various image qualities and resolutions (584×354 to 1945×1181), lasting 10-42 seconds.
- Endo NeRF [183]: Contains two surgical video clips, one with 63 frames and the other with 156 frames, focusing on endoscopic image analysis. SUN-SEG [186] is the first high-quality video polyp segmentation dataset, containing 158,690 colonoscopy video frames with various annotation types. SurgToolLoc [184]: Comprising 24,695 30-second video clips at 60 fps, this dataset is used for endoscopic image analysis, with tool presence annotations and bounding box labels in the test set.
- YouTube-VOS [178] is a large-scale dataset with 4,453 clips in 94 object categories, including humans, animals, and vehicles. It addresses spatio-temporal challenges and includes complex multi-object scenes, with 3,471 training and 507 validation videos for evaluating model performance.
- VOT-LT Series [180], [182] is specialized for long-term video tracking tasks, containing 50 and 52 videos, respectively. It provides a large data volume with persistent targets, making it suitable for evaluating long-term stability and robustness. VOT-ST Series [182], [187]

TABLE 7: Detailed summary of video datasets, including the year of publication, publication venue, number of videos, frames, duration, objects, annotation type, and tasks.

Dataset	Year	Pub.	Videos	Frames	Duration	Objects	Annotation	Tasks
SegTrack [170]	2012	IJCV	6	-	-	6	244	Segmentation and Tracking
SegTrack-v2 [171]	2013	ICCV	14	976	-	24	1154	Segmentation and Tracking
YouTube-Objects [172]	2013	CVPR	126	-	-	96	2153	Weakly-supervised learning
FBMS-59 [173]	2014	TPAMI	59	13860	7.7(min)	139	1465	Motion Segmentation
Jump-cut [174]	2015	CVPR	22	-	-	22	6331	Video Cutout
DAVIS16 [30]	2016	CVPR	50	3455	2.5(min)	50	3455	Video Object Segmentation
DAVIS17 [175]	2017	arxiv	90	10700	5.17(min)	205	13543	Video Object Segmentation
EndoVis17 [176]	2017	MICCAI	8	2040	-	7	-	Robotic Instrument Segmentation
EndoVis18 [177]	2018	MICCAI	10	3000	-	10	-	Instrument and Anatomical
YouTube-VOS [178]	2018	ECCV	4453	120532	334.8(min)	7755	197272	Video object segmentation
CAMUS [179]	2019	TMI	1000	-	-	-	-	Ultrasound
VOT-LT 2019 [180]	2019	ICCV	50	215298	119(min)	50	215298	Object Tracking
UVO [181]	2021	CVPR	1200	~ 108000	511(min)	14748	~ 1327000	open-world, class-agnostic
VOT-LT 2022 [182]	2022	ECCV	52	168282	93(min)	50	168282	Object Tracking
Endo NeRF [183]	2022	MICCAI	6	807	0.6(min)	-	-	Surgical scene reconstruction
SurgToolLoc [184]	2022	MICCAI	24695	1481700	205.8(h)	11	-	Surgical Tool Localization
VIPSeg [185]	2022	CVPR	3536	-	353.6(min)	124	84750	Video Panoptic Segmentation
SUN-SEG [186]	2022	MIR	113	158,690	11.3(min)	-	-	Video polyp segmentation
VOT-ST 2022 [182]	2022	ECCV	62	19903	11.1(min)	62	19826	Object Tracking
VOT-ST 2023 [187]	2023	ICCV	144	298640	166(min)	341	-	Tracking and Segmentation
VOST [188]	2023	CVPR	713	75547	252(min)	-	175913	Object transformation segmentation
BURST [189]	2023	WACV	2914	624240	1734(min)	16089	600157	Tracking and segmentation
MOSE [190]	2023	ICCV	2149	~159600	443.6(min)	5200	431725	Complex scene object segmentation
PUMaVOS [191]	2023	ICCV	24	-	11.6(min)	-	21K	Challenging segmentation
ESD [192]	2023	Arxiv	120	14563	-	-	14166	Event-based object segmentation
MeViS [193]	2023	ICCV	2006	-	-	8171	443K	Motion-guided Segmentation
PolypGen [194]	2023	Sci.Data	1537	6500	-	-	3762	Polyp detection
LVOS-V1 [195]	2023	ICCV	220	126280	351(min)	282	156432	Long video segmentation
LVOS-V2 [196]	2024	arxiv	720	296401	823(min)	1132	407945	Long video segmentation
SA-V [16]	2024	CVPR	50.9K	4.2M	196h	-	642.6K	Multiple scenes and details

focuses on short-term tracking, with the 2023 version expanding to 144 videos and nearly 300,000 frames with finer annotations, supporting multi-object segmentation in dynamic scenes.

- ESD [192] is the first 3D spatio-temporal event segmentation dataset, featuring 145 sequences and 21.88 million events for occluded object segmentation. VIPSeg [185] is the first large-scale outdoor video panoptic segmentation dataset, containing 3,536 videos and 84,750 frames of pixel-level annotations.
- VOST [188] is a semi-supervised video object segmentation benchmark focused on complex object deformations. It includes targets that break, tear, or undergo significant shape changes. The dataset consists of over 700 high-resolution video clips, averaging 20 seconds each, with dense instance mask annotations. It is designed to capture the complete deformation process, offering challenging scenarios for VOS models.
- UVO [181] and BURST [189] are large-scale multi-object segmentation datasets with 1,200 and 2,914 videos, respectively. UVO offers 14,748 objects with over 1.32 million annotations, focusing on undefined object segmentation. BURST covers 482 object categories and 600,157 annotations, serving as a critical resource for ultra-long video tasks.
- MOSE [190] is a video object segmentation (VOS) dataset for complex real-world scenarios, containing 2,149 video clips and providing 43,725 high-quality segmentation masks across multi-object scenes. The dataset is divided into 1,507 training videos, 311 validation videos, and 331 test videos, covering 36 categories with a total of 5,200 objects. PUMaVOS [191] is a video object segmentation dataset that covers partial and unusual objects, consisting of 24 video clips and 21K densely annotated frames. It focuses on partial objects (such as half faces, necks, tattoos) commonly retouched in film production, suitable for segmentation tasks in complex scenes.
- MeViS [193] is a large-scale video segmentation dataset focused on motion expression-guided object segmentation. It contains 2,006 videos covering complex multi-object scenes, selected through rigorous visual and linguistic criteria, with detailed language expression annotations to advance motion-guided video segmentation research. PolypGen [194] is a large-scale dataset with 3,762 annotated polyp labels from over 300 patients across six independent centers. It includes both single-frame and sequence data, with precise polyp boundary delineation, aimed at advancing colon polyp detection and pixel-level segmentation research.
- LVOS [195] is a long-term video object segmentation dataset designed for real-world scenes, featuring videos averaging over 60 seconds. It includes 720 videos in v1 and 420 in v2 [196], with 44 categories, providing

challenges like object reappearance. The dataset is split into training, validation, and test videos to evaluate model generalization.

- Segment Anything Video (SA-V) [16] is a large-scale dataset with 50,900 clips and 642,600 masks for prompt-based video segmentation. It covers challenges like small objects and occlusion, with data divided into training, validation, and test sets. This dataset supports robust model development and provides a platform for evaluating segmentation algorithms.

4.3 Evaluate Metrics

Video segmentation, which involves temporal data, introduces additional complexity compared to image segmentation, particularly in the temporal dimension, placing higher demands on the stability, consistency, and continuity of segmentation algorithms. While image segmentation typically focuses on pixel classification within a single frame, video segmentation must ensure both spatial segmentation and temporal coherence, avoiding issues like object jitter or drift across frames. Therefore, when evaluating video segmentation performance, it is essential not only to use common metrics such as IoU and Dice but also to consider the impact of the temporal dimension to comprehensively assess both the spatial and temporal aspects of the segmentation results.

The following metrics described in [30], [175] are commonly used evaluation metrics for video segmentation.

4.3.1 Region Similarity \mathcal{J} and Contour Precision \mathcal{F}

Given the predicted segmentation masks $\hat{M} \in \{0, 1\}^{H \times W}$ and the ground truth masks $M \in \{0, 1\}^{H \times W}$, the **region similarity** \mathcal{J} is computed as the Intersection-over-Union (IoU) between \hat{M} and M :

$$\mathcal{J} = \frac{\hat{M} \cap M}{\hat{M} \cup M}. \quad (5)$$

To assess the contour quality of \hat{M} , we calculate the contour recall R_c and precision P_c using bipartite graph matching [197]. The **contour accuracy** \mathcal{F} is then defined as the harmonic mean of contour recall R_c and precision P_c :

$$\mathcal{F} = \frac{2P_cR_c}{P_c + R_c}. \quad (6)$$

This metric quantifies how closely the contours of the predicted masks align with those of the ground-truth masks. The average contour accuracy, $\mathcal{F}_{\text{mean}}$, is computed across all objects. For brevity, we denote this by \mathcal{F} .

Finally, the overall performance is measured using the **combined metric** $\mathcal{J\&F}$, which is the arithmetic mean of the region similarity and contour accuracy:

$$\mathcal{J\&F} = \frac{\mathcal{J} + \mathcal{F}}{2}. \quad (7)$$

4.3.2 Global Accuracy

The \mathcal{G} **metric (Global Accuracy)** is used to measure the overall accuracy of segmentation results. It is defined as the proportion of correctly classified pixels in the predicted segmentation to the total number of pixels. The formula is:

$$\mathcal{G} = \frac{\text{Number of correctly classified pixels}}{\text{Total number of pixels}}. \quad (8)$$

Intuitively, \mathcal{G} reflects the overall proportion of correctly classified pixels. A higher \mathcal{G} value indicates better global segmentation accuracy.

4.3.3 Temporal Metrics: FPS

FPS (Frames Per Second) is a temporal metric (add cite) used to evaluate the processing speed of a video segmentation or analysis model. It measures the number of video frames that the model can process per second, reflecting its efficiency and suitability for real-time applications. A higher FPS indicates that the model can handle video data more quickly, making it ideal for time-sensitive tasks.

$$FPS = \frac{\text{Number of Frames Processed}}{\text{Time Taken (in seconds)}}. \quad (9)$$

5 DISCUSSION

During the development of this paper, we observed that SAM2 shows significant improvements compared to previous models, demonstrating great potential. However, despite these advancements, there are still several challenges and limitations that require further research and refinement. In this section, we will discuss the current challenges and opportunities in this field.

5.1 Current Challenges

5.1.1 Domain Adaptation Limitations

Although SAM2 performs well in zero-shot tasks [124], [164], its application in domains such as medical imaging and remote sensing still requires domain-specific fine-tuning to achieve optimal performance. These fields often rely on complex contextual information [73], and the model's generalization ability is limited without targeted data. The fine-tuning process faces challenges such as high computational costs and insufficiently labeled data, particularly for specialized tasks. These issues highlight the ongoing need for efficient domain adaptation techniques and the generation of high-quality labeled datasets.

5.1.2 Multimodal Integration

Another significant challenge lies in the efficient integration of SAM2 with multimodal models. SAM2 has the potential to process multimodal data, such as combining image features with textual descriptions, but the effective fusion of these data types remains a complex task [165], [198]. Multimodal integration requires sophisticated mechanisms to align and merge data from different sources, which can be computationally intensive and may involve dealing with differences in modality-specific feature spaces. Furthermore, the model needs to effectively leverage information from diverse inputs while maintaining performance across all modalities. Future research must focus on improving multimodal interaction capabilities to ensure that SAM2 can process and understand complex multimodal data streams in a cohesive manner.

5.1.3 Inference Speed and Resource Requirements

SAM2, being a large and complex model, faces significant challenges [166], [199] when it comes to real-time applications, such as video segmentation and online segmentation systems. Due to its large size, SAM2 can experience slower inference times and higher resource consumption, which can hinder its deployment in environments where speed and efficiency are critical. In particular, tasks such as video segmentation, which require processing multiple frames per second, demand a high degree of computational power and low latency. Addressing these challenges will require optimization techniques that reduce the model's computational overhead while maintaining performance. Efficient resource management will be key to enabling SAM2's practical use in real-time applications, such as autonomous driving and live video analysis.

5.2 Future Works

Future work will focus on optimizing model performance, enhancing multimodal interaction capabilities, and improving robustness to address challenges in real-world applications.

5.2.1 Fine-Tuning for Specialized Field

Develop more efficient fine-tuning strategies [54] tailored to specific domains (e.g., medical imaging, remote sensing) to enhance the model's adaptability and performance. By leveraging domain-specific data and task-optimized techniques, the model can better address real-world applications, achieving higher precision in segmentation tasks.

5.2.2 Lightweight Optimization

Reduce the computational overhead of the model through techniques such as model pruning and knowledge distillation, thereby improving inference efficiency. Further optimize the model structure to ensure high performance even in resource-constrained scenarios, particularly for real-time applications [163], [200], [201].

5.2.3 Enhanced Multimodal Interaction

Investigate deeper integration of SAM2 with multimodal data inputs, such as language descriptions and textual information [47], [51], [202], to explore its potential application scenarios. By enhancing multimodal interaction, the model can be applied more effectively to complex and diverse tasks, including intelligent question answering and image-text analysis.

5.2.4 Improving Robustness

Incorporate a wider variety of complex and diverse datasets during training to improve the model's ability to handle challenging scenarios such as noise and occlusion [169], [203]. Techniques such as data augmentation and adversarial training can further enhance the model's stability and reliability under uncertain conditions.

6 CONCLUSION

This paper reviews the advances and challenges of SAM2 in the field of image and video segmentation. Compared to its predecessor, SAM2 shows significant improvements in handling complex scenarios, though its performance in specific domains such as medical imaging and autonomous driving still requires further optimization. The study focuses on SAM2's applications in image and video segmentation: in the image domain, it emphasizes its capabilities in medical image processing; in the video domain, it highlights its handling of temporal consistency. Despite existing challenges, the technological potential of SAM2 offers valuable directions for future research and practical applications. We hope that the insights provided in this paper will serve as a useful reference for researchers, driving the continued optimization and broader adoption of SAM2 in the field of computer vision.

REFERENCES

- [1] R. Szeliski, *Computer vision: algorithms and applications*. Nature, 2022.
- [2] H. Li, X. Zhao, A. Su, H. Zhang, J. Liu, and G. Gu, "Color space transformation and multi-class weighted loss for adhesive white blood cell segmentation," *IEEE access*, 2020.
- [3] S. Zhou, D. Nie, E. Adeli, J. Yin, J. Lian, and D. Shen, "High-resolution encoder-decoder networks for low-contrast medical image segmentation," *IEEE TIP*, 2019.
- [4] X. E. Pantazi, D. Moshou, and A. A. Tamouridou, "Automated leaf disease detection in different crop species through image features analysis and one class classifiers," *Computers and electronics in agriculture*, 2019.
- [5] S. Y. Lee, B. A. Tama, S. J. Moon, and S. Lee, "Steel surface defect diagnostics using deep convolutional neural network and class activation map," *Applied Sciences*, 2019.
- [6] M. Cordts, M. Omran, S. Ramos, T. Rehfeld, M. Enzweiler, R. Benenson, U. Franke, S. Roth, and B. Schiele, "The cityscapes dataset for semantic urban scene understanding," in *CVPR*, 2016.
- [7] Y. Wang, Q. Qi, L. Jiang, and Y. Liu, "Hybrid remote sensing image segmentation considering intrasegment homogeneity and intersegment heterogeneity," *IEEE Geoscience and Remote Sensing Letters*, 2019.
- [8] L. Zhang, J. Ma, X. Lv, and D. Chen, "Hierarchical weakly supervised learning for residential area semantic segmentation in remote sensing images," *IEEE Geoscience and Remote Sensing Letters*, 2019.
- [9] X. Wang, G. Chen, G. Qian, P. Gao, X.-Y. Wei, Y. Wang, Y. Tian, and W. Gao, "Large-scale multi-modal pre-trained models: A comprehensive survey," *Machine Intelligence Research*, vol. 20, no. 4, pp. 447–482, 2023.
- [10] A. Kirillov, E. Mintun, N. Ravi, H. Mao, C. Rolland, L. Gustafson, T. Xiao, S. Whitehead, A. C. Berg, W.-Y. Lo *et al.*, "Segment anything," in *ICCV*, 2023.
- [11] S. Sengupta, S. Chakrabarty, and R. Soni, "Is sam 2 better than sam in medical image segmentation?" *arXiv:2408.04212*, 2024.
- [12] J. Ma, Y. He, F. Li, L. Han, C. You, and B. Wang, "Segment anything in medical images," *Nature Communications*, 2024.
- [13] J. Ye, J. Cheng, J. Chen, Z. Deng, T. Li, H. Wang, Y. Su, Z. Huang, J. Chen, L. Jiang *et al.*, "Sa-med2d-20m dataset: Segment anything in 2d medical imaging with 20 million masks," *arXiv:2311.11969*, 2023.
- [14] C. Chen, J. Miao, D. Wu, A. Zhong, Z. Yan, S. Kim, J. Hu, Z. Liu, L. Sun, X. Li *et al.*, "Ma-sam: Modality-agnostic sam adaptation for 3d medical image segmentation," *Elsevier MIA*, 2024.
- [15] P. Guo, Z. Zhao, J. Gao, C. Wu, T. He, Z. Zhang, T. Xiao, and W. Zhang, "Videosam: Open-world video segmentation," *arXiv:2410.08781*, 2024.
- [16] N. Ravi, V. Gabeur, Y.-T. Hu, R. Hu, C. Ryali, T. Ma, H. Khedr, R. Rädle, C. Rolland, L. Gustafson *et al.*, "Sam 2: Segment anything in images and videos," *arXiv:2408.00714*, 2024.

- [17] Y. Zhang and R. Jiao, "Towards segment anything model (sam) for medical image segmentation: a survey," *arXiv:2305.03678*, 2023.
- [18] C. Zhang, L. Liu, Y. Cui, G. Huang, W. Lin, Y. Yang, and Y. Hu, "A comprehensive survey on segment anything model for vision and beyond," *arXiv:2305.08196*, 2023.
- [19] Y. Zhang and Z. Shen, "Unleashing the potential of sam2 for biomedical images and videos: A survey," *arXiv:2408.12889*, 2024.
- [20] Y. Zhou, G. Sun, Y. Li, L. Benini, and E. Konukoglu, "When sam2 meets video camouflaged object segmentation: A comprehensive evaluation and adaptation," *arXiv:2409.18653*, 2024.
- [21] X. Sun, J. Liu, H. T. Shen, X. Zhu, and P. Hu, "On efficient variants of segment anything model: A survey," *arXiv:2410.04960*, 2024.
- [22] C. Zhang, Y. Cui, W. Lin, G. Huang, Y. Rong, L. Liu, and S. Shan, "Segment anything for videos: A systematic survey," *arXiv:2408.08315*, 2024.
- [23] L.-C. Chen, "Semantic image segmentation with deep convolutional nets and fully connected crfs," *arXiv:1412.7062*, 2014.
- [24] —, "Rethinking atrous convolution for semantic image segmentation," *arXiv:1706.05587*, 2017.
- [25] L.-C. Chen, Y. Zhu, G. Papandreou, F. Schroff, and H. Adam, "Encoder-decoder with atrous separable convolution for semantic image segmentation," in *ECCV*, 2018.
- [26] A. M. Hafiz and G. M. Bhat, "A survey on instance segmentation: state of the art," *International journal of multimedia information retrieval*, 2020.
- [27] S. Liu, L. Qi, H. Qin, J. Shi, and J. Jia, "Path aggregation network for instance segmentation," in *CVPR*, 2018.
- [28] D. Bolya, C. Zhou, F. Xiao, and Y. J. Lee, "Yolact: Real-time instance segmentation," in *ICCV*, 2019.
- [29] A. Kirillov, K. He, R. Girshick, C. Rother, and P. Dollár, "Panoptic segmentation," in *CVPR*, 2019.
- [30] F. Perazzi, J. Pont-Tuset, B. McWilliams, L. Van Gool, M. Gross, and A. Sorkine-Hornung, "A benchmark dataset and evaluation methodology for video object segmentation," in *CVPR*, 2016.
- [31] T. Zhou, F. Porikli, D. J. Crandall, L. Van Gool, and W. Wang, "A survey on deep learning technique for video segmentation," *IEEE TPAMI*, 2022.
- [32] R. Bommasani, D. A. Hudson, E. Adeli, R. Altman, S. Arora, S. von Arx, M. S. Bernstein, J. Bohg, A. Bosselut, E. Brunskill *et al.*, "On the opportunities and risks of foundation models," *arXiv:2108.07258*, 2021.
- [33] L. Yuan, D. Chen, Y.-L. Chen, N. Codella, X. Dai, J. Gao, H. Hu, X. Huang, B. Li, C. Li *et al.*, "Florence: A new foundation model for computer vision," *arXiv:2111.11432*, 2021.
- [34] A. Radford, J. W. Kim, C. Hallacy, A. Ramesh, G. Goh, S. Agarwal, G. Sastry, A. Askell, P. Mishkin, J. Clark *et al.*, "Learning transferable visual models from natural language supervision," in *ICML*, 2021.
- [35] D. Alexey, "An image is worth 16x16 words: Transformers for image recognition at scale," *arXiv: 2010.11929*, 2020.
- [36] K. Han, Y. Wang, H. Chen, X. Chen, J. Guo, Z. Liu, Y. Tang, A. Xiao, C. Xu, Y. Xu *et al.*, "A survey on vision transformer," *IEEE TPAMI*, 2022.
- [37] K. He, X. Chen, S. Xie, Y. Li, P. Dollár, and R. Girshick, "Masked autoencoders are scalable vision learners," in *CVPR*, 2022.
- [38] M. Tancik, P. Srinivasan, B. Mildenhall, S. Fridovich-Keil, N. Raghavan, U. Singhal, R. Ramamoorthi, J. Barron, and R. Ng, "Fourier features let networks learn high frequency functions in low dimensional domains," 2020.
- [39] A. Vaswani, "Attention is all you need," 2017.
- [40] T. Dao, "Flashattention-2: Faster attention with better parallelism and work partitioning," *arXiv:2307.08691*, 2023.
- [41] A. S. Geetha and M. Hussain, "From sam to sam 2: Exploring improvements in meta's segment anything model," *arXiv:2408.06305*, 2024.
- [42] Y. Liu, Y. Zhao, X. Zhang, X. Wang, C. Lian, J. Li, P. Shan, C. Fu, X. Lyu, L. Li *et al.*, "Mobilesam-track: Lightweight one-shot tracking and segmentation of small objects on edge devices," *Remote Sensing*, vol. 15, no. 24, p. 5665, 2023.
- [43] H. Dai, C. Ma, Z. Yan, Z. Liu, E. Shi, Y. Li, P. Shu, X. Wei, L. Zhao, Z. Wu *et al.*, "Samaug: Point prompt augmentation for segment anything model," *arXiv:2307.01187*, 2023.
- [44] R. Zhang, Z. Jiang, Z. Guo, S. Yan, J. Pan, X. Ma, H. Dong, P. Gao, and H. Li, "Personalize segment anything model with one shot," *arXiv:2305.03048*, 2023.
- [45] T. Chen, L. Zhu, C. Deng, R. Cao, Y. Wang, S. Zhang, Z. Li, L. Sun, Y. Zang, and P. Mao, "Sam-adapter: Adapting segment anything in underperformed scenes," in *ICCV*, 2023.
- [46] J. Cheng, B. Fu, J. Ye, G. Wang, T. Li, H. Wang, R. Li, H. Yao, J. Chen, J. Li *et al.*, "Interactive medical image segmentation: A benchmark dataset and baseline," *arXiv:2411.12814*, 2024.
- [47] D. Li, W. Xie, M. Cao, Y. Wang, J. Zhang, Y. Li, L. Fang, and C. Xu, "Fusionsam: Latent space driven segment anything model for multimodal fusion and segmentation," *arXiv:2408.13980*, 2024.
- [48] N. Liu, X. Xu, Y. Su, H. Zhang, and H.-C. Li, "Pointsam: Pointly-supervised segment anything model for remote sensing images," *arXiv:2409.13401*, 2024.
- [49] J. Xu, X. Li, C. Yue, Y. Wang, and Y. Guo, "Sam-mpa: Applying sam to few-shot medical image segmentation using mask propagation and auto-prompting," *arXiv:2411.17363*, 2024.
- [50] A. Xiao, W. Xuan, H. Qi, Y. Xing, R. Ren, X. Zhang, L. Shao, and S. Lu, "Cat-sam: Conditional tuning for few-shot adaptation of segment anything model," in *ECCV*, 2024.
- [51] Y. Zhang, T. Cheng, R. Hu, L. Liu, H. Liu, L. Ran, X. Chen, W. Liu, and X. Wang, "Evf-sam: Early vision-language fusion for text-prompted segment anything model," *arXiv:2406.20076*, 2024.
- [52] J. Zhu, Y. Qi, and J. Wu, "Medical sam 2: Segment medical images as video via segment anything model 2," *arXiv:2408.00874*, 2024.
- [53] Z. Yan, W. Sun, R. Zhou, Z. Yuan, K. Zhang, Y. Li, T. Liu, Q. Li, X. Li, L. He *et al.*, "Biomedical sam 2: Segment anything in biomedical images and videos," *arXiv:2408.03286*, 2024.
- [54] X. Chen, C. Wang, H. Ning, M. Zhang, M. Shen, and S. Li, "Sam-octa2: Layer sequence octa segmentation with fine-tuned segment anything model 2," *arXiv:2409.09286*, 2024.
- [55] J. Qiu, W. Liu, E. Li, L. Zhang, and X. Li, "Ded-sam: Adapting segment anything model 2 for dual encoder-decoder change detection," *IEEE Journal of Selected Topics in Applied Earth Observations and Remote Sensing*, 2024.
- [56] T. Chen, A. Lu, L. Zhu, C. Ding, C. Yu, D. Ji, Z. Li, L. Sun, P. Mao, and Y. Zang, "Sam2-adapter: Evaluating & adapting segment anything 2 in downstream tasks: Camouflage, shadow, medical image segmentation, and more," *arXiv:2408.04579*, 2024.
- [57] M. Zhang, L. Wang, Z. Chen, Y. Ge, and X. Tao, "Path-sam2: Transfer sam2 for digital pathology semantic segmentation," *arXiv:2408.03651*, 2024.
- [58] F. Isensee, P. F. Jaeger, S. A. Kohl, J. Petersen, and K. H. Maier-Hein, "nnu-net: a self-configuring method for deep learning-based biomedical image segmentation," *Nature methods*, 2021.
- [59] J. Chen, Y. Lu, Q. Yu, X. Luo, E. Adeli, Y. Wang, L. Lu, A. L. Yuille, and Y. Zhou, "Transunet: Transformers make strong encoders for medical image segmentation," *arXiv:2102.04306*, 2021.
- [60] V. I. Butoi, J. J. G. Ortiz, T. Ma, M. R. Sabuncu, J. Guttag, and A. V. Dalca, "Universeg: Universal medical image segmentation," in *ICCV*, 2023.
- [61] Q. Wei, H. Zhang, and J.-H. Yong, "Focused and collaborative feedback integration for interactive image segmentation," in *CVPR*, 2023.
- [62] Z. Yan, T. Han, Y. Huang, L. Liu, H. Zhou, J. Chen, W. Shi, Y. Cao, X. Yang, and D. Ni, "A foundation model for general moving object segmentation in medical images," in *ISBI*, 2024.
- [63] H. K. Cheng and A. G. Schwing, "Xmem: Long-term video object segmentation with an atkinson-shiffrin memory model," in *ECCV*, 2022.
- [64] J. Wu, R. Fu, H. Fang, Y. Zhang, Y. Yang, H. Xiong, H. Liu, and Y. Xu, "Medsegdiff: Medical image segmentation with diffusion probabilistic model," in *Medical Imaging with Deep Learning*. PMLR, 2024, pp. 1623–1639.
- [65] J. Wu and M. Xu, "One-prompt to segment all medical images," in *CVPR*, 2024.
- [66] H. Dong, H. Gu, Y. Chen, J. Yang, Y. Chen, and M. A. Mazurowski, "Segment anything model 2: an application to 2d and 3d medical images," *arXiv:2408.00756*, 2024.
- [67] C. Shen, W. Li, Y. Shi, and X. Wang, "Interactive 3d medical image segmentation with sam 2," *arXiv:2408.02635*, 2024.
- [68] Y. He, P. Guo, Y. Tang, A. Myronenko, V. Nath, Z. Xu, D. Yang, C. Zhao, D. Xu, and W. Li, "A short review and evaluation of sam2's performance in 3d ct image segmentation," *arXiv:2408.11210*, 2024.
- [69] X. Xiong, Z. Wu, S. Tan, W. Li, F. Tang, Y. Chen, S. Li, J. Ma, and G. Li, "Sam2-unet: Segment anything 2 makes strong encoder for natural and medical image segmentation," *arXiv:2408.08870*, 2024.

- [70] J. Ma, S. Kim, F. Li, M. Baharoon, R. Asakereh, H. Lyu, and B. Wang, "Segment anything in medical images and videos: Benchmark and deployment," *arXiv:2408.03322*, 2024.
- [71] Y. Yamagishi, S. Hanaoka, T. Kikuchi, T. Nakao, Y. Nakamura, Y. Nomura, S. Miki, T. Yoshikawa, and O. Abe, "Zero-shot 3d segmentation of abdominal organs in ct scans using segment anything model 2: Adapting video tracking capabilities for 3d medical imaging," *arXiv e-prints*, pp. arXiv-2408, 2024.
- [72] Z. Yildiz, Y. Chen, and M. A. Mazurowski, "Sam & sam 2 in 3d slicer: Segmentwithsam extension for annotating medical images," *arXiv:2408.15224*, 2024.
- [73] X. Zhao, Y. Pang, S. Chang, Y. Zhao, L. Zhang, H. Lu, J. Ouyang, G. E. Fakhri, and X. Liu, "Inspiring the next generation of segment anything models: Comprehensively evaluate sam and sam 2 with diverse prompts towards context-dependent concepts under different scenes," *arXiv:2412.01240*, 2024.
- [74] J. Hong, M. Fulton, and J. Sattar, "Trashcan: A semantically-segmented dataset towards visual detection of marine debris," *arXiv:2007.08097*, 2020.
- [75] C. Trotter, G. Atkinson, M. Sharpe, K. Richardson, A. S. McGough, N. Wright, B. Burville, and P. Berggren, "Ndd20: A large-scale few-shot dolphin dataset for coarse and fine-grained categorisation," *arXiv:2005.13359*, 2020.
- [76] Z. Ziqiang, X. Yaofeng, L. Haixin, Y. Zhibin, and S.-K. Yeung, "Coralvos: Dataset and benchmark for coral video segmentation," *arXiv:2310.01946*, 2023.
- [77] M. Minervini, A. Fischbach, H. Scharr, and S. A. Tsaftaris, "Finely-grained annotated datasets for image-based plant phenotyping," *Elsevier PRL*, 2016.
- [78] J. A. Cruz, X. Yin, X. Liu, S. M. Imran, D. D. Morris, D. M. Kramer, and J. Chen, "Multi-modality imagery database for plant phenotyping," *Springer MVA*, 2016.
- [79] H. Uchiyama, S. Sakurai, M. Mishima, D. Arita, T. Okayasu, A. Shimada, and R.-i. Taniguchi, "An easy-to-setup 3d phenotyping platform for komatsuna dataset," in *ICCVW*, 2017.
- [80] J. Xiao, J. Hays, K. A. Ehinger, A. Oliva, and A. Torralba, "Sun database: Large-scale scene recognition from abbey to zoo," in *CVPR*, 2010.
- [81] T.-Y. Lin, M. Maire, S. Belongie, J. Hays, P. Perona, D. Ramanan, P. Dollár, and C. L. Zitnick, "Microsoft coco: Common objects in context," in *ECCV*, 2014.
- [82] M. Cordts, M. Omran, S. Ramos, T. Rehfeld, M. Enzweiler, R. Benenson, U. Franke, S. Roth, and B. Schiele, "The cityscapes dataset for semantic urban scene understanding," in *CVPR*, 2016.
- [83] B. Zhou, A. Lapedriza, A. Khosla, A. Oliva, and A. Torralba, "Places: A 10 million image database for scene recognition," *IEEE TPAMI*, 2017.
- [84] B. Zhou, H. Zhao, X. Puig, T. Xiao, S. Fidler, A. Barriuso, and A. Torralba, "Semantic understanding of scenes through the ade20k dataset," *Springer IJCV*, 2019.
- [85] A. Gupta, P. Dollar, and R. Girshick, "Lvis: A dataset for large vocabulary instance segmentation," in *CVPR*, 2019.
- [86] C. Snyder and M. Do, "Streets: A novel camera network dataset for traffic flow," *NeurIPS*, 2019.
- [87] L. Yang, Y. Z. Wei, Y. He, W. Sun, Z. Huang, H. Huang, and H. Fan, "ishape: A first step towards irregular shape instance segmentation," *arXiv:2109.15068*, 2021.
- [88] L. Ciampi, C. Santiago, J. Costeira, C. Gennaro, and G. Amato, "Night and day instance segmented park (ndis-park) dataset: a collection of images taken by day and by night for vehicle detection, segmentation and counting in parking areas," *Zenodo*, vol. 8, p. 18, 2022.
- [89] L. Ciampi, C. Santiago, J. P. Costeira, C. Gennaro, and G. Amato, "Domain adaptation for traffic density estimation." in *VISIGRAPP (5: VISAPP)*, 2021, pp. 185–195.
- [90] J. Chen, Y. Xu, S. Lu, R. Liang, and L. Nan, "3-d instance segmentation of mvs buildings," *IEEE TGRS*, 2022.
- [91] Y. Li, Z. Ye, and J. M. Rehg, "Delving into egocentric actions," in *CVPR*, 2015.
- [92] A. Darkhalil, D. Shan, B. Zhu, J. Ma, A. Kar, R. Higgins, S. Fidler, D. Fouhey, and D. Damen, "Epic-kitchens visor benchmark: Video segmentations and object relations," *NeurIPS*, 2022.
- [93] L. Zhang, S. Zhou, S. Stent, and J. Shi, "Fine-grained egocentric hand-object segmentation: Dataset, model, and applications," in *ECCV*, 2022.
- [94] N. Cohen, Y. Newman, and A. Shamir, "Semantic segmentation in art paintings," in *Computer graphics forum*, vol. 41, no. 2. Wiley Online Library, 2022, pp. 261–275.
- [95] Q. Hu, W. Zhou, X. Peng, X. Zhang, P. Xie, Y. Liu, J. Peng, and J. Fan, "Dragnet: A semantic segmentation network for chinese landscape paintings," *Digital Signal Processing*, vol. 147, p. 104427, 2024.
- [96] R. Yang, H. Yang, M. Zhao, R. Jia, X. Wu, and Y. Zhang, "Special perceptual parsing for chinese landscape painting scene understanding: a semantic segmentation approach," *Neural Computing and Applications*, vol. 36, no. 10, pp. 5231–5249, 2024.
- [97] B. Kim, C. Shin, J. Jeong, H. Jung, S.-Y. Lee, S. Chun, D.-H. Hwang, and J. Yu, "Zim: Zero-shot image matting for anything," *arXiv:2411.00626*, 2024.
- [98] J. C. Caicedo, A. Goodman, K. W. Karhohs, B. A. Cimini, J. Ackerman, M. Haghghi, C. Heng, T. Becker, M. Doan, C. McQuin *et al.*, "Nucleus segmentation across imaging experiments: the 2018 data science bowl," *Nature methods*, vol. 16, no. 12, pp. 1247–1253, 2019.
- [99] S. Yogamani, C. Hughes, J. Horgan, G. Sistu, P. Varley, D. O'Dea, M. Uricár, S. Milz, M. Simon, K. Amende *et al.*, "Woodscape: A multi-task, multi-camera fisheye dataset for autonomous driving," in *ICCV*, 2019.
- [100] M. Pugliatti and F. Topputo, "Doors: Dataset for boulders segmentation," *Zenodo*, vol. 9, no. 20, p. 6, 2022.
- [101] J.-M. Fortin, O. Gamache, V. Grondin, F. Pomerleau, and P. Giguère, "Instance segmentation for autonomous log grasping in forestry operations," in *IROS*, 2022.
- [102] M. Roberts, J. Ramapuram, A. Ranjan, A. Kumar, M. A. Bautista, N. Paczan, R. Webb, and J. M. Susskind, "Hypersim: A photorealistic synthetic dataset for holistic indoor scene understanding," in *ICCV*, 2021.
- [103] T. Haucke, H. S. Kühl, and V. Steinhage, "Socrates: Introducing depth in visual wildlife monitoring using stereo vision," *MDPI Sensors*, 2022.
- [104] D. Bashkirova, M. Abdelfattah, Z. Zhu, J. Akl, F. Alladkani, P. Hu, V. Ablavsky, B. Calli, S. A. Bargal, and K. Saenko, "Zerowaste dataset: Towards deformable object segmentation in cluttered scenes," in *CVPR*, 2022.
- [105] J. Qi, Y. Gao, Y. Hu, X. Wang, X. Liu, X. Bai, S. Belongie, A. Yuille, P. H. Torr, and S. Bai, "Occluded video instance segmentation: A benchmark," *IJCV*, 2022.
- [106] B. H. Menze, A. Jakab, S. Bauer, J. Kalpathy-Cramer, K. Farahani, J. Kirby, Y. Burren, N. Porz, J. Slotboom, R. Wiest *et al.*, "The multimodal brain tumor image segmentation benchmark (brats)," *IEEE TMI*, 2014.
- [107] M. Boccardi, M. Bocchetta, F. C. Morency, D. L. Collins, M. Nishikawa, R. Ganzola, M. J. Grothe, D. Wolf, A. Redolfi, M. Pievani *et al.*, "Training labels for hippocampal segmentation based on the eadc-adni harmonized hippocampal protocol," *Alzheimer's & Dementia*, 2015.
- [108] A. L. Simpson, M. Antonelli, S. Bakas, M. Bilello, K. Farahani, B. Van Ginneken, A. Kopp-Schneider, B. A. Landman, G. Litjens, B. Menze *et al.*, "A large annotated medical image dataset for the development and evaluation of segmentation algorithms," *arXiv:1902.09063*, 2019.
- [109] V. Oreiller, V. Andrearczyk, M. Jreige, S. Boughdad, H. Elhalawani, J. Castelli, M. Vallières, S. Zhu, J. Xie, Y. Peng *et al.*, "Head and neck tumor segmentation in pet/ct: the hecktor challenge," *Elsevier MIA*, 2022.
- [110] H. Gong, J. Chen, G. Chen, H. Li, G. Li, and F. Chen, "Thyroid region prior guided attention for ultrasound segmentation of thyroid nodules," *Computers in biology and medicine*, 2023.
- [111] S. Jaeger, S. Candemir, S. Antani, Y.-X. J. Wang, P.-X. Lu, and G. Thoma, "Two public chest x-ray datasets for computer-aided screening of pulmonary diseases," *Quantitative imaging in medicine and surgery*, vol. 4, no. 6, p. 475, 2014.
- [112] A. M. Tahir, M. E. Chowdhury, A. Khandakar, T. Rahman, Y. Qiblawey, U. Khurshid, S. Kiranyaz, N. Ibtihaz, M. S. Rahman, S. Al-Maadeed *et al.*, "Covid-19 infection localization and severity grading from chest x-ray images," *Computers in biology and medicine*, 2021.
- [113] W. Al-Dhabyani, M. Goma, H. Khaled, and A. Fahmy, "Dataset of breast ultrasound images," *Data in brief*, vol. 28, p. 104863, 2020.
- [114] —, "Dataset of breast ultrasound images," *Data in brief*, vol. 28, p. 104863, 2020.

- [115] Z. Xiong, Q. Xia, Z. Hu, N. Huang, C. Bian, Y. Zheng, S. Vesal, N. Ravikumar, A. Maier, X. Yang *et al.*, "A global benchmark of algorithms for segmenting the left atrium from late gadolinium-enhanced cardiac magnetic resonance imaging," *Elsevier MIA*, 2021.
- [116] H. Choi, N. Dahiya, and S. Nadeem, "Cirdataset: a large-scale dataset for clinically-interpretable lung nodule radiomics and malignancy prediction," in *MICCAI*, 2022.
- [117] L. Zhao, X. Chen, E. Z. Chen, Y. Liu, T. Chen, and S. Sun, "Retrieval-augmented few-shot medical image segmentation with foundation models," *arXiv:2408.08813*, 2024.
- [118] M. A. Attiyeh, J. Chakraborty, A. Doussot, L. Langdon-Embry, S. Mainerich, M. Gönen, V. P. Balachandran, M. I. D'Angelica, R. P. DeMatteo, W. R. Jarnagin *et al.*, "Survival prediction in pancreatic ductal adenocarcinoma by quantitative computed tomography image analysis," *Annals of surgical oncology*, vol. 25, pp. 1034–1042, 2018.
- [119] D. Jha, P. H. Smedsrud, M. A. Riegler, P. Halvorsen, T. De Lange, D. Johansen, and H. D. Johansen, "Kvasir-seg: A segmented polyp dataset," in *MultiMedia modeling: 26th international conference, MMM 2020*. Springer, 2020.
- [120] Y. Song, J. Zheng, L. Lei, Z. Ni, B. Zhao, and Y. Hu, "Ct2us: Cross-modal transfer learning for kidney segmentation in ultrasound images with synthesized data," *Ultrasonics*, vol. 122, p. 106706, 2022.
- [121] P. Bilic, P. Christ, H. B. Li, E. Vorontsov, A. Ben-Cohen, G. Kaissis, A. Szeskin, C. Jacobs, G. E. H. Mamani, G. Chartrand *et al.*, "The liver tumor segmentation benchmark (lits)," *Elsevier MIA*, 2023.
- [122] Q. Liu, Q. Dou, L. Yu, and P. A. Heng, "Ms-net: multi-site network for improving prostate segmentation with heterogeneous mri data," *IEEE TMI*, 2020.
- [123] Q. Zhao, S. Lyu, W. Bai, L. Cai, B. Liu, M. Wu, X. Sang, M. Yang, and L. Chen, "A multi-modality ovarian tumor ultrasound image dataset for unsupervised cross-domain semantic segmentation," *arXiv:2207.06799*, 2022.
- [124] A. S. Yu, M. Hariri, X. Zhang, M. Yang, V. Chaudhary, and X. Li, "Novel adaptation of video segmentation to 3d mri: efficient zero-shot knee segmentation with sam2," *arXiv:2408.04762*, 2024.
- [125] F. Prados, J. Ashburner, C. Blaiotta, T. Brosch, J. Carballido-Gamio, M. J. Cardoso, B. N. Conrad, E. Datta, G. Dávid, B. De Leener *et al.*, "Spinal cord grey matter segmentation challenge," *Neuroimage*, vol. 152, pp. 312–329, 2017.
- [126] S. Pang, C. Pang, L. Zhao, Y. Chen, Z. Su, Y. Zhou, M. Huang, W. Yang, H. Lu, and Q. Feng, "Spinearsenet: spine parsing for volumetric mr image by a two-stage segmentation framework with semantic image representation," *IEEE TMI*, 2020.
- [127] A. Sekuboyina, M. E. Hussein, A. Bayat, M. Löffler, H. Liebl, H. Li, G. Tetteh, J. Kukačka, C. Payer, D. Štern *et al.*, "Verse: a vertebrae labelling and segmentation benchmark for multi-detector ct images," *Elsevier MIA*, 2021.
- [128] N. C. Codella, D. Gutman, M. E. Celebi, B. Helba, M. A. Marchetti, S. W. Dusza, A. Kalloo, K. Liopyris, N. Mishra, H. Kittler *et al.*, "Skin lesion analysis toward melanoma detection: A challenge at the 2017 isbi, hosted by the isic," in *ISBI*, 2018.
- [129] S. Gatidis, T. Hepp, M. Früh, C. La Fougère, K. Nikolaou, C. Pfannenbergh, B. Schölkopf, T. Küstner, C. Cyran, and D. Rubin, "A whole-body fdg-pet/ct dataset with manually annotated tumor lesions," *Scientific Data*, vol. 9, no. 1, p. 601, 2022.
- [130] M. R. Hernandez Petzsche, E. de la Rosa, U. Hanning, R. Wiest, W. Valenzuela, M. Reyes, M. Meyer, S.-L. Liew, F. Kofler, I. Ezhov *et al.*, "Isles 2022: A multi-center magnetic resonance imaging stroke lesion segmentation dataset," *Scientific data*, 2022.
- [131] A. Hakim, S. Christensen, S. Winzeck, M. G. Lansberg, M. W. Parsons, C. Lucas, D. Robben, R. Wiest, M. Reyes, and G. Zaharchuk, "Predicting infarct core from computed tomography perfusion in acute ischemia with machine learning: Lessons from the isles challenge," *Stroke*, 2021.
- [132] Y. Huang, X. Yang, L. Liu, H. Zhou, A. Chang, X. Zhou, R. Chen, J. Yu, J. Chen, C. Chen *et al.*, "Segment anything model for medical images?" *Elsevier MIA*, 2024.
- [133] Y. Hu, T. Li, Q. Lu, W. Shao, J. He, Y. Qiao, and P. Luo, "Om-nimedvqa: A new large-scale comprehensive evaluation benchmark for medical lvlm," in *CVPR*, 2024.
- [134] K. Sirinukunwattana, J. P. Pluim, H. Chen, X. Qi, P.-A. Heng, Y. B. Guo, L. Y. Wang, B. J. Matuszewski, E. Bruni, U. Sanchez *et al.*, "Gland segmentation in colon histology images: The glas challenge contest," *Elsevier MIA*, 2017.
- [135] T. L. van den Heuvel, D. de Bruijn, C. L. de Korte, and B. v. Ginneken, "Automated measurement of fetal head circumference using 2d ultrasound images," *PLoS one*, vol. 13, no. 8, p. e0200412, 2018.
- [136] S. Graham, H. Chen, J. Gamper, Q. Dou, P.-A. Heng, D. Snead, Y. W. Tsang, and N. Rajpoot, "Mild-net: Minimal information loss dilated network for gland instance segmentation in colon histology images," *Elsevier MIA*, 2019.
- [137] M. Li, K. Huang, Q. Xu, J. Yang, Y. Zhang, Z. Ji, K. Xie, S. Yuan, Q. Liu, and Q. Chen, "Octa-500: a retinal dataset for optical coherence tomography angiography study," *Elsevier MIA*, 2024.
- [138] L. Shi, X. Li, W. Hu, H. Chen, J. Chen, Z. Fan, M. Gao, Y. Jing, G. Lu, D. Ma *et al.*, "Ebhi-seg: A novel endoscopy biopsy histopathological hematoxylin and eosin image dataset for image segmentation tasks," *Frontiers in Medicine*, 2023.
- [139] C. Wang, A. Mahbod, I. Ellinger, A. Galdran, S. Gopalakrishnan, J. Niezgod, and Z. Yu, "Fuseg: The foot ulcer segmentation challenge," *Information*, 2024.
- [140] E. Gibson, F. Giganti, Y. Hu, E. Bonmati, S. Bandula, K. Gurusamy, B. Davidson, S. P. Pereira, M. J. Clarkson, and D. C. Barratt, "Automatic multi-organ segmentation on abdominal ct with dense v-networks," *IEEE TMI*, 2018.
- [141] B. Rister, K. Shivakumar, T. Nobashi, and D. L. Rubin, "Ct-org: Ct volumes with multiple organ segmentations [dataset]," *The Cancer Imaging Archive*, vol. 21, 2019.
- [142] X. Fang and P. Yan, "Multi-organ segmentation over partially labeled datasets with multi-scale feature abstraction," *IEEE TMI*, 2020.
- [143] J. Ma, Y. Zhang, S. Gu, C. Zhu, C. Ge, Y. Zhang, X. An, C. Wang, Q. Wang, X. Liu *et al.*, "Abdomenct-1k: Is abdominal organ segmentation a solved problem?" *IEEE TPAMI*, 2021.
- [144] A. E. Kavur, N. S. Gezer, M. Barış, S. Aslan, P.-H. Conze, V. Groza, D. D. Pham, S. Chatterjee, P. Ernst, S. Özkan *et al.*, "Chaos challenge-combined (ct-mr) healthy abdominal organ segmentation," *Elsevier MIA*, 2021.
- [145] J. Ma, Y. Zhang, S. Gu, C. Ge, S. Ma, A. Young, C. Zhu, K. Meng, X. Yang, Z. Huang *et al.*, "Unleashing the strengths of unlabeled data in pan-cancer abdominal organ quantification: the flare22 challenge," *arXiv:2308.05862*, 2023.
- [146] Y. Ji, H. Bai, C. Ge, J. Yang, Y. Zhu, R. Zhang, Z. Li, L. Zhanng, W. Ma, X. Wan *et al.*, "Amos: A large-scale abdominal multi-organ benchmark for versatile medical image segmentation," *NeurIPS*, 2022.
- [147] J. Wasserthal, H.-C. Breit, M. T. Meyer, M. Pradella, D. Hinck, A. W. Sauter, T. Heye, D. T. Boll, J. Cyriac, S. Yang *et al.*, "Totalsegmentator: robust segmentation of 104 anatomic structures in ct images," *Radiology: Artificial Intelligence*, vol. 5, no. 5, 2023.
- [148] H. K. Cheng, Y.-W. Tai, and C.-K. Tang, "Rethinking space-time networks with improved memory coverage for efficient video object segmentation," 2021.
- [149] X. Wang, X. Zhang, Y. Cao, W. Wang, C. Shen, and T. Huang, "Seggpt: Segmenting everything in context," *arXiv:2304.03284*, 2023.
- [150] Z. Yang and Y. Yang, "Decoupling features in hierarchical propagation for video object segmentation," 2022.
- [151] M. Li, L. Hu, Z. Xiong, B. Zhang, P. Pan, and D. Liu, "Recurrent dynamic embedding for video object segmentation," in *CVPR*, 2022.
- [152] S. W. Oh, J.-Y. Lee, N. Xu, and S. J. Kim, "Video object segmentation using space-time memory networks," in *ICCV*, 2019.
- [153] H. K. Cheng, S. W. Oh, B. Price, A. Schwing, and J.-Y. Lee, "Tracking anything with decoupled video segmentation," in *ICCV*, 2023.
- [154] L. Hong, W. Chen, Z. Liu, W. Zhang, P. Guo, Z. Chen, and W. Zhang, "Lvos: A benchmark for long-term video object segmentation," in *ICCV*, 2023.
- [155] H. K. Cheng, S. W. Oh, B. Price, J.-Y. Lee, and A. Schwing, "Putting the object back into video object segmentation," in *CVPR*, 2024.
- [156] Q. Liu, J. Wang, Z. Yang, L. Li, K. Lin, M. Niethammer, and L. Wang, "Livros: Light video object segmentation with gated linear matching," *arXiv:2411.02818*, 2024.
- [157] F. Rajić, L. Ke, Y.-W. Tai, C.-K. Tang, M. Danelljan, and F. Yu, "Segment anything meets point tracking," *arXiv:2307.01197*, 2023.
- [158] W. Yue, J. Zhang, K. Hu, Y. Xia, J. Luo, and Z. Wang, "Surgic-sam: Efficient class promptable surgical instrument segmentation," in *AAAI*, 2024.

- [159] X. Deng, H. Wu, R. Zeng, and J. Qin, "Memsam: Taming segment anything model for echocardiography video segmentation," in *CVPR*, 2024.
- [160] T. Zhou, W. Luo, Q. Ye, Z. Shi, and J. Chen, "Sam-pd: How far can sam take us in tracking and segmenting anything in videos by prompt denoising," *arXiv:2403.04194*, 2024.
- [161] S. Xu, H. Yuan, Q. Shi, L. Qi, J. Wang, Y. Yang, Y. Li, K. Chen, Y. Tong, B. Ghanem *et al.*, "Rap-sam: Towards real-time all-purpose segment anything," *arXiv:2401.10228*, 2024.
- [162] M. Mansoori, S. Shahabodini, J. Abouei, K. N. Plataniotis, and A. Mohammadi, "Self-prompting polyp segmentation in colonoscopy using hybrid yolo-sam 2 model," *arXiv:2409.09484*, 2024.
- [163] H. Liu, E. Zhang, J. Wu, M. Hong, and Y. Jin, "Surgical sam 2: Real-time segment anything in surgical video by efficient frame pruning," *arXiv:2408.07931*, 2024.
- [164] M. Mansoori, S. Shahabodini, J. Abouei, K. N. Plataniotis, and A. Mohammadi, "Polyp sam 2: Advancing zero shot polyp segmentation in colorectal cancer detection," *arXiv:2408.05892*, 2024.
- [165] C. Cuttano, G. Trivigno, G. Rosi, C. Masone, and G. Averta, "Samwise: Infusing wisdom in sam2 for text-driven video segmentation," *arXiv:2411.17646*, 2024.
- [166] Z. Wang, Q. Zhou, and Z. Liu, "Det-sam2: Technical report on the self-prompting segmentation framework based on segment anything model 2," *arXiv:2411.18977*, 2024.
- [167] C.-Y. Yang, H.-W. Huang, W. Chai, Z. Jiang, and J.-N. Hwang, "Samurai: Adapting segment anything model for zero-shot visual tracking with motion-aware memory," *arXiv:2411.11922*, 2024.
- [168] S. Ding, R. Qian, X. Dong, P. Zhang, Y. Zang, Y. Cao, Y. Guo, D. Lin, and J. Wang, "Sam2long: Enhancing sam 2 for long video segmentation with a training-free memory tree," *arXiv:2410.16268*, 2024.
- [169] Y. Shen, H. Ding, X. Shao, and M. Unberath, "Performance and non-adversarial robustness of the segment anything model 2 in surgical video segmentation," *arXiv:2408.04098*, 2024.
- [170] D. Tsai, M. Flagg, A. Nakazawa, and J. M. Rehg, "Motion coherent tracking using multi-label mrf optimization," *IJCV*, 2012.
- [171] F. Li, T. Kim, A. Humayun, D. Tsai, and J. M. Rehg, "Video segmentation by tracking many figure-ground segments," in *ICCV*, 2013.
- [172] A. Prest, C. Leistner, J. Civera, C. Schmid, and V. Ferrari, "Learning object class detectors from weakly annotated video," in *CVPR*, 2012.
- [173] P. Ochs, J. Malik, and T. Brox, "Segmentation of moving objects by long term video analysis," *IEEE TPAMI*, 2013.
- [174] Q. Fan, F. Zhong, D. Lischinski, D. Cohen-Or, and B. Chen, "Jumpcut: non-successive mask transfer and interpolation for video cutout." *ACM Trans. Graph.*, vol. 34, no. 6, pp. 195–1, 2015.
- [175] J. Pont-Tuset, F. Perazzi, S. Caelles, P. Arbeláez, A. Sorkine-Hornung, and L. Van Gool, "The 2017 davis challenge on video object segmentation," *arXiv:1704.00675*, 2017.
- [176] M. Allan, A. Shvets, T. Kurmann, Z. Zhang, R. Duggal, Y.-H. Su, N. Rieke, I. Laina, N. Kalavakonda, S. Bodenstedt *et al.*, "2017 robotic instrument segmentation challenge," *arXiv:1902.06426*, 2019.
- [177] M. Allan, S. Kondo, S. Bodenstedt, S. Leger, R. Kadkhodamohammadi, I. Luengo, F. Fuentes, E. Flouty, A. Mohammed, M. Pedersen *et al.*, "2018 robotic scene segmentation challenge," *arXiv:2001.11190*, 2020.
- [178] N. Xu, L. Yang, Y. Fan, J. Yang, D. Yue, Y. Liang, B. Price, S. Cohen, and T. Huang, "Youtube-vos: Sequence-to-sequence video object segmentation," in *ECCV*, 2018.
- [179] S. Leclerc, E. Smistad, A. Østvik, F. Cervenansky, F. Espinosa, T. Espeland, E. A. R. Berg, P.-M. Jodoin, T. Grenier, C. Lartizien *et al.*, "Deep learning segmentation in 2d echocardiography using the camus dataset: Automatic assessment of the anatomical shape validity," *arXiv:1908.02994*, 2019.
- [180] M. Kristan, J. Matas, A. Leonardis, M. Felsberg, R. Pflugfelder, J.-K. Kamarainen, L. Čehovin Zajc, O. Drbohlav, A. Lukežič, A. Berg *et al.*, "The seventh visual object tracking vot2019 challenge results," in *ICCVW*, 2019.
- [181] W. Wang, M. Feiszli, H. Wang, and D. Tran, "Unidentified video objects: A benchmark for dense, open-world segmentation," in *ICCV*, 2021.
- [182] M. Kristan, A. Leonardis, J. Matas, M. Felsberg, R. Pflugfelder, J.-K. Kamarainen, H. J. Chang, M. Danelljan, L. Č. Zajc, A. Lukežič *et al.*, "The tenth visual object tracking vot2022 challenge results," in *ECCV*, 2022.
- [183] Y. Wang, Y. Long, S. H. Fan, and Q. Dou, "Neural rendering for stereo 3d reconstruction of deformable tissues in robotic surgery," in *MICCAI*, 2022.
- [184] A. Zia, K. Bhattacharyya, X. Liu, M. Berniker, Z. Wang, R. Nespolo, S. Kondo, S. Kasai, K. Hirasawa, B. Liu *et al.*, "Surgical tool classification and localization: results and methods from the miccai 2022 surgtoolloc challenge," *arXiv:2305.07152*, 2023.
- [185] J. Miao, X. Wang, Y. Wu, W. Li, X. Zhang, Y. Wei, and Y. Yang, "Large-scale video panoptic segmentation in the wild: A benchmark," in *CVPR*, 2022.
- [186] G.-P. Ji, G. Xiao, Y.-C. Chou, D.-P. Fan, K. Zhao, G. Chen, and L. Van Gool, "Video polyp segmentation: A deep learning perspective," *Springer MIR*, 2022.
- [187] M. Kristan, J. Matas, M. Danelljan, M. Felsberg, H. J. Chang, L. Č. Zajc, A. Lukežič, O. Drbohlav, Z. Zhang, K.-T. Tran *et al.*, "The first visual object tracking segmentation vots2023 challenge results," in *ICCV*, 2023.
- [188] P. Tokmakov, J. Li, and A. Gaidon, "Breaking the "object" in video object segmentation," in *CVPR*, 2023.
- [189] A. Athar, J. Luiten, P. Voigtlaender, T. Khurana, A. Dave, B. Leibe, and D. Ramanan, "Burst: A benchmark for unifying object recognition, segmentation and tracking in video," in *Proceedings of the IEEE/CVF winter conference on applications of computer vision*, 2023, pp. 1674–1683.
- [190] H. Ding, C. Liu, S. He, X. Jiang, P. H. Torr, and S. Bai, "Mose: A new dataset for video object segmentation in complex scenes," in *ICCV*, 2023.
- [191] M. Bekuzarov, A. Bermudez, J.-Y. Lee, and H. Li, "Xmem++: Production-level video segmentation from few annotated frames," in *ICCV*, 2023.
- [192] X. Huang, K. Sanket, A. Ayyad, F. B. Naeini, D. Makris, and Y. Zweiri, "A neuromorphic dataset for object segmentation in indoor cluttered environment," *arXiv:2302.06301*, 2023.
- [193] H. Ding, C. Liu, S. He, X. Jiang, and C. C. Loy, "Mevis: A large-scale benchmark for video segmentation with motion expressions," in *ICCV*, 2023.
- [194] S. Ali, D. Jha, N. Ghatwary, S. Realdon, R. Cannizzaro, O. E. Salem, D. Lamarque, C. Daul, M. A. Riegler, K. V. Anonsen *et al.*, "A multi-centre polyp detection and segmentation dataset for generalisability assessment," *Scientific Data*, vol. 10, no. 1, p. 75, 2023.
- [195] L. Hong, W. Chen, Z. Liu, W. Zhang, P. Guo, Z. Chen, and W. Zhang, "Lvos: A benchmark for long-term video object segmentation," in *ICCV*, 2023.
- [196] L. Hong, Z. Liu, W. Chen, C. Tan, Y. Feng, X. Zhou, P. Guo, J. Li, Z. Chen, S. Gao *et al.*, "Lvos: A benchmark for large-scale long-term video object segmentation," *arXiv:2404.19326*, 2024.
- [197] D. R. Martin, C. C. Fowlkes, and J. Malik, "Learning to detect natural image boundaries using local brightness, color, and texture cues," *IEEE TPAMI*, 2004.
- [198] J. Huo, S. Ourselin, and R. Sparks, "Sam-i2i: Unleash the power of segment anything model for medical image translation," *arXiv:2411.12755*, 2024.
- [199] C. Zhang, F. D. Puspitasari, S. Zheng, C. Li, Y. Qiao, T. Kang, X. Shan, C. Zhang, C. Qin, F. Rameau *et al.*, "A survey on segment anything model (sam): Vision foundation model meets prompt engineering," *arXiv:2306.06211*, 2023.
- [200] J. Yu, A. Wang, W. Dong, M. Xu, M. Islam, J. Wang, L. Bai, and H. Ren, "Sam 2 in robotic surgery: An empirical evaluation for robustness and generalization in surgical video segmentation," *arXiv:2408.04593*, 2024.
- [201] R. Lu, S. Shi, Y. Liu, and D. Wang, "Samedge: An edge-cloud video analytics architecture for the segment anything model," *arXiv:2409.14784*, 2024.
- [202] C. Zhu, B. Xiao, L. Shi, S. Xu, and X. Zheng, "Customize segment anything model for multi-modal semantic segmentation with mixture of lora experts," *arXiv:2412.04220*, 2024.
- [203] O. Rafaeli, T. Svoray, R. Blushtein-Livnon, and A. Nahlieli, "Prompt-based segmentation at multiple resolutions and lighting conditions using segment anything model 2," *arXiv:2408.06970*, 2024.